

Response to Reviewer Comments**Date: 2020-05-11****By R. Reese, A. Levermann, T. Albrecht, H. Seroussi and R. Winkelmann**

Journal: TC

Title: The role of history and strength of the oceanic forcing in sea-level projections from Antarctica with the Parallel Ice Sheet Model

Author(s): R.Reese, A.Levermann, T.Albrecht, H.Seroussi and R.Winkelmann

MS No.: tc-2019-330

MS Type: Research article

First of all, we would like to thank the editor Douglas Brinkerhoff and the two anonymous reviewers for their helpful and excellent comments. We provide detailed replies to all comments below, with our responses indicated in blue. Line numbers refer to the revised version of the manuscript.

Anonymous referee 1

Received and published: 21 February 2020

Interactive comment on The Cryosphere Discuss., <https://doi.org/10.5194/tc-2019-330-RC1>, 2020**General comments:**

This paper describes the sensitivity of ice-sheet projections to the initialization method (simulating the 1850-2014 historical period vs starting in 2015, after the same long spin-up in both cases). It also describes the sensitivity to ocean warming, and compares the effect of parameterised melting (through PICO in ISMIP6 simulations) to melt perturbations imposed in LARMIP2. These sensitivities are expressed as Antarctic contributions to sea level rise.

The paper is well written, although a few clarifications are required in the Methods section. While I find the results useful for the ice-sheet/climate community, I have a few major comments that should probably be addressed before publishing this paper:

We would like to thank the anonymous reviewer for his/her effort to review our manuscript and greatly appreciate his/her comments for improving our study.

1. An important conclusion of this paper appears to be that ice-sheet models should simulate the entire historical period to make meaningful projections. However, this would not be true if the initial state was selected in a way to get present-day thinning rates (e.g. including an observational ice thinning rate in the score used to pick the initial state in the long-term ensemble). I don't expect the authors to change this in their methodology, but this should be discussed.

Thanks for making the suggestion to add thinning rates to the scoring system - we want to consider this in the future as also discussed in the specific comments. Since in the initial ensemble we run the members for several thousand years with constant climate conditions towards equilibrium, we think that ideally this would be combined with a historic simulation that yields correct thinning rates for present-day, i.e., making ‘hindcasting’ experiments.

We believe that getting thinning rates correctly in the initial state would substantially improve projections. However, due to the non-linearity of the equation system, this might not be fully sufficient. For example, appropriate estimates of the three-dimensional temperature field would be required.

We added this to the discussion in Section 4.3. For a detailed discussion of the effects of the historic simulation, please see the reply to the last comment of reviewer 2.

2. A strong ad hoc temperature correction is applied to the Amundsen Sea, with deep-ocean temperatures set to -1.25°C , i.e. relatively cold conditions. Then, it is claimed that the PICO tuning parameters cannot be changed because they were tuned to match observational ice-shelf averaged melt rates (in Reese et al. 2018 with other ocean forcing dataset). These aspects need to be investigated in this paper. Melting (and ideally the ice-sheet response) without temperature correction should be described, and other tuning parameters should be considered. Further, it could be argued that the important observational target in terms of ice-shelf buttressing is not the ice-shelf average but the average in PICO’s first box (near grounding line).

Many thanks for pointing us to this inconsistency. In line with Jourdain et al. (view) and Seroussi et al. (view), a central finding of this manuscript is that the tuning of basal melt rate parameterisations should be reconsidered for future projections of sea-level rise. Using a temperature correction in the tuning is one approach that we plan to explore in the future also for other basins than the Amundsen Sea. We changed the text correspondingly in lines 154ff and lines 285ff. We agree that tuning the parameterisation to obtain sub-shelf melt rates in PICO’s first box would be a great addition for future work, as well as considering melt rate variability and temperature corrections (added in lines 288f).

Table 1: Amundsen Sea ocean temperature T , average basal melt rates \dot{m} and melt rate sensitivity $\Delta\dot{m}$, calculated from one degree of ocean warming.

Experiment	year	T ($^{\circ}\text{C}$)	\dot{m} (m a^{-1})	$\Delta\dot{m}$ ($\text{m a}^{-1} \text{ } ^{\circ}\text{C}^{-1}$)
Pseudo steady-state	1850 or 2014	-1.25	4.9	8.3
After historic	2014	-0.65	9.9	8.6
WOA 2018 pre-release	1955-2018	0.85	23.1	9.2
Schmidtke	1975-2012	0.45	19.9	9.1

To estimate the effects of the temperature correction in the Amundsen Sea, we calcu-

lated the melt rate and melt rate sensitivity with and without the temperature correction (Table 1 here). The different initial ocean conditions in the Amundsen Sea yield different basin-wide average melt rates. However, as also shown in Figure 7 of the manuscript, the melt-rate sensitivities in PICO are (especially for warmer temperatures) mostly linear. Hence, basal melt rate changes are predominantly controlled by temperature changes and less by initial temperatures which means that our results are not much influenced by the temperature correction applied in the Amundsen Sea.

We show a constant-climate simulation for 5,000 years with the ‘warm’ ocean conditions

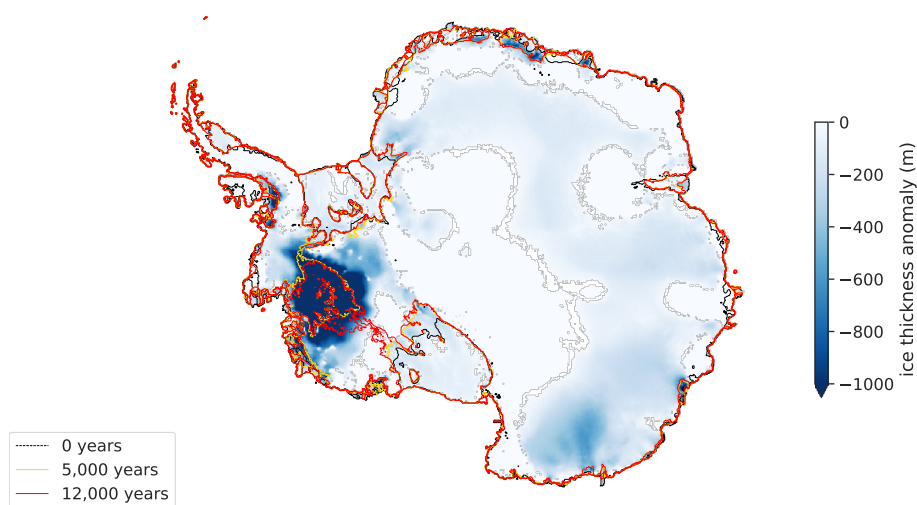


Figure 1: Ice thickness change and grounding line movement for warm Amundsen Sea conditions. The simulation is similar to the pseudo-steady-state reference configuration, except that Amundsen Sea temperatures are at the warm, present-day values. Results are similar for all members of the initial ensemble.

for comparison (see Fig. 1 here) as well as projections for different PICO parameter (see Fig. 2 of this response). Using ‘warm’ ocean conditions in the Amundsen Sea in the initial ensemble, we find for all ensemble members, that the WAIS starts to collapse. Given that the current imbalance of the Amundsen Sea region is likely caused by the ocean, we think that for the initialisation procedure employed in this study, a reduction of ocean conditions to ‘cold’ is a feasible assumption: this correction does not mean that PICO produces overly high melt rates for the Amundsen Sea region (average melt rates are in line with observations, see Reese et al. (2018) and Table 1 of this response) or that PISM cannot handle observed melt rates. The response of PISM to melt rates close to present-day in the Amundsen sea is a collapse of that region over several thousand years of constant climate forcing (see Figure 1 of this response). With this region is out of balance today, creating

a steady state with present-day ocean conditions would require to tune parameters to be overly stable. This is also in line with other model studies (e.g., Favier et al., 2014). This is discussed in detail in the reply to the specific comment on lines 99-100.

We test for different PICO parameters by re-running projections forced with NorESM1-M (Fig. 2) with increased parameter values. We find that, depending on the parameters, mass loss increases substantially. This is in comparison to control simulations which show a large drift since the initial setup is not close to equilibrium with the new parameters. For future sea-level projections, a thorough re-assessment of the parameters would be necessary.

Please see also the detailed reply to the specific comment below and to the corresponding comment by Reviewer 2.

3. Melt rates obtained through the ISMIP6 framework are compared to the melt rates imposed in LARMIP2 (based on previous plume-model studies). It would be interesting to describe how these two types of melt rates compared to other observational or modelling studies (see specific comment below).

Thanks for mentioning this. Please see the response to the specific comment on Section 4.2 below.

Specific comments:

- L. 43-45: These are global feedbacks related to freshwater injection into the ocean. There are also important local thickness-melting feedbacks described by Timmermann and Goeller (2017) and Donat-Magnin et al. (2017).

Many thanks for pointing us to these two relevant studies.

- L. 51: ‘haven’ -> ‘have’. Done.

Section 2.1: I don’t necessarily ask the authors to do it, but it would be interesting to see the score of the historical simulation in 2015 compared to the ensemble of initial states and in particular the one that was selected against present-day observations of ice geometry and speed.

Please see the new Supplementary Figure 1 in which we added the historic simulation to the scoring. It scores slightly worse than the selected configuration. As you mention below, using present-day thinning rates would be a helpful measure to test the historic simulation, which is not reflected in the current scores. Please see also the reply to the respective comment by Reviewer 2.

- L. 81: About ‘scoring against present-day observations of ice geometry’: including the ice thinning rate in the score would have helped get an initial state similar to observations and maybe to the historic state at 2015.

This is a good idea that we will add for future studies.

L. 89-90: What constant value is used for 1850 – 1949?

We added an explanation in lines 130f. Note that the used, aggregated, yearly surface mass balance is very similar to the RACMO climatology as shown in the historic versus the ctrl*-simulation in Fig. S3.

L. 90-91: This sentence is unclear.

Please see the changed text (lines 134-140) and the response to the respective comment by Reviewer 2.

Section 2.2: Specify here what is done for SMB in LARMIP-2. Done.

L. 96-97: ‘ $C = 106$ ’ would be better than programming notation. And both C and γ_T should have units. The γ_T value does not seem to be exactly the same as Reese et al. (2018), why has it been modified despite a careful tuning in that paper?

We changed the notation of C and added units.

The value of γ_T was part of the initial ensemble. We added this to the manuscript in lines 90ff as well as a Supplementary Figure showing the scores of the ensemble. The range of γ_T in the ensemble has been based on Reese et al. (2018), where diagnostic experiments were done to tune the parameters. We here found that in transient simulations the higher value to yield a better initial configuration. However, as we discuss also in the response to your major comments, this value yields sensitivities lower than the ones used in LARMIP-2. A re-evaluation of the basal melt rate sensitivity and an alternative tuning approach might be needed. Note that the findings for the Amundsen Sea region (major comment 2) were consistent for all values of γ_T in the initial ensemble.

L. 98-99: How was the data compilation based on World Ocean Atlas (WOA) 2018 and Schmidtko’s dataset built? Was the latest update of WOA 2018 used? If not it is worth being mentioned because there were important updates near Antarctica.

See <https://www.nodc.noaa.gov/OC5/woa18/woa18data.html>

Thanks for pointing this out. We did use the pre-release of WOA2018 and added this correspondingly as well as a more detailed description of how the data from WOA2018-prerelease and (Schmidtko et al., 2014) were processed and combined. The exact procedure is described in the Bachelor Thesis by Lena Nicola (2019) - we are happy to send it to everyone interested.

L. 99-100: Changing the Amundsen Sea temperatures to -1.25°C is quite an issue. Does it mean that PICO produces overly high melt rates in the Amundsen Sea, or that PISM cannot handle melt rates close to observational estimates? In Levermann et al. (2020), a similar correction is done to -0.37°C with a claim that this possibly represents pre-industrial conditions. This needs to be discussed, and what’s happening for uncorrected temperatures needs to be shown in this paper. It is a crucial point because (1) the Amundsen Sea is our

best present-day test for future warm conditions, and (2) the small sensitivity reported in this paper with the ISMIP6 framework could be due to this artificial cooling in the Amundsen Sea.

Thanks for bringing up these points which is very important. This is an ad-hoc correction to reduce Amundsen Sea temperatures to ‘cold’ conditions that we discuss in the following and in lines 154ff of the revised manuscript. As explained in our reply to the general comment 2, this does not mean that PICO produces overly high melt rates for the Amundsen Sea region.

Concerning (1): especially because the Amundsen Sea is our best present-day test for warm conditions and since observations show that the Amundsen Sea is out of balance at the moment, we argue that reducing ocean temperatures in the Amundsen sea is important due to the initialisation procedure of our experiments (see above). Furthermore, we think that observations of the Amundsen Sea melt rates would be very valuable for assessing PICO’s melt rate sensitivity in a next step.

Concerning (2): note that in PICO, the changes in basal melt rates are mostly dependent on the changes in ocean temperatures and not so much on the initial ocean temperature, since the sensitivity of basal melt rates to ocean temperatures is mostly linear. This is true especially for larger ocean temperatures, see Figure 7 in the manuscript and Figure 6 in Reese et al. (2018). Please note that over the historic simulation, Amundsen Sea temperatures increase by 0.6°C , see Table 1 in this response, so that the projections based on the historic simulation start from warmer ocean conditions in the Amundsen Sea.

We agree with the reviewer that the correction of temperatures as well as the melt rate sensitivity should be further assessed in a new tuning approach for basal melt rate parameterisations for projections of Antarctica’s future mass loss.

Please see also the reply to your major comment 2 and the respective comment by Reviewer 2.

- L. 103: Is NorESM1-M used from 1850 onward? I don’t understand what is the ‘new climatology’ and how it is used.

Similar to the atmosphere forcing, we apply NorESM1-M ocean forcing in the historic simulation. To account for changes in the ocean temperatures and salinity over the historic simulation, we initialize the projections based on the historic simulation from a new climatology. This climatology is obtained from the 1995-2014 average conditions in the historic simulation, to make sure that we do not start simulation, e.g. the control run, from exceptionally high or low values at the end of 2014 that arise from interannual variability in the forcing (see Fig. S3).

Note that we decided to start the historic simulation from the same conditions as the pseudo-steady state which means that atmospheric and oceanic boundary conditions in 2015 differ between the two configurations. However, this allows to start from two states

that are very similar (see lines 103ff) and avoids running two ensembles with different boundary conditions, one with present-day conditions and one with scaled historic conditions. Since changes over the historic simulation are small, see Fig. S3 we expect this to have a minor effect.

We added an explanation in lines 161f.

- L. 104: Not clear, what ‘ISMIP6 ocean forcing’ refers to? It has just been explained that PICO is used, ‘initialized with an ocean data compilation from Locarnini et al. (2018) and Schmidtke et al. (2014)’, with additional CMIP5 anomalies. Is there anything else to add?

We wanted to make clear that the projections are run with ocean forcing only. We added a new section (2.2) to describe the experiments in order to clarify this.

- Arriving at section 3, it is surprising to see several CMIP5 models while only NorESM1-M was mentioned in section 2. The use of several models (all starting from NorESM1-M’s 1850-2014 period) should be described in section 2. The methods should be understandable without knowing the full ISMIP6 framework.

We added a new subsection (2.2) and a table S1 to describe the experiments in more detail.

- L. 124: ‘basal mass balance increased’ or basal mass balance DEcreased? Same in Tab. 1, should SMB and BMB have the same sign for ice-sheet mass loss? Maybe just a matter of taste... Done.

Section 3.1: it might be clearer to define the ‘ctrl’ experiment in section 2, and to explain how it is designed: which part of the historical forcing is kept constant until 2100?

We added a description in the new subsection ‘experiments’ of Section 2.

Tab.1 and Sect. 3.2: please briefly define ‘asmb’ and ‘abmb’ so that it can be understood without having to read Seroussi et al. (2019).

Explained in the new section ‘experiments’.

Throughout Sect. 3: In view of the drifts in ctrl vs ctrl*, it is expected to see different mass loss for the two initialisations. All the plots and mass loss estimates could be calculated with respect to ctrl or ctrl*... Done.

- L. 146: you could cite Edwards et al. (2019) here as it revisits several previous estimates. Done.

L.147: it is difficult to visualise the 50%. You could consider redo Fig. 2 with ctrl and ctrl* subtracted.

Mass loss in Figure 2 is shown with respect to ctrl or ctrl*, respectively. We hope that this clarifies the comment?

Section 3.4: The differences between the initial state used for PISM-PIK in Levermann et al. (2020) and the one used for LARMIP-2 PISM simulations should be summarised somewhere in this manuscript. Without this it is difficult to understand what to expect from this section. We added a detailed comparison of the PISM-PIK contributions for LARMIP-2 and ISMIP6 to the Supplementary Information (new Table S2) and refer to it in line 212f.

Section 4.1: here only NorESM1-M results are shown because it ‘shows highest mass losses of all ISMIP6 experiments’. This is true for the total Antarctic mass loss, but the results considering individual sectors (as in Fig. 4) may be higher in other models. Furthermore, LARMIP-2 is based on a CMIP5 19-model mean, so it seems more appropriate to use the ISMIP6 multi-model mean here rather than just NorESM1-M.

Thanks for raising this point. We added in Fig. 4 and 5 basal melt rates and mass loss in all regions for the other RCP8.5 simulations following the ISMIP6 protocol that we present in this manuscript. Since basal melt rate forcing and mass loss in the experiments driven by CCSM and MIROC are overall similar to NorESM1-M, we can generalize our findings to these models. We would expect the multi-model mean of these models to yield similar results.

One interesting feature that arises when comparing the CMIP5-forcings is that basal melt rate changes in East Antarctica seem similar in Figure 4 for NorESM1-M and MIROC but mass loss is higher for NorESM1-M as shown in Figure 5. This is because ocean forcing in the ISMIP6 simulations varies across the different ice shelves in East Antarctica, but is constant for LARMIP-2. While there is stronger ocean warming in Dronning Maud Land and Amery in the MIROC forcing, the ocean warms substantially more in the Totten region for NorESM1-M. Since the Totten region is more vulnerable to ocean warming, melt rate increases in that area cause larger overall mass losses.

We added a description in lines 254ff.

L.224-225: It is true that tuning C and γ_T would ‘affect the comparison of sub-shelf melt rates to present-day observations’. But (1) the input temperatures have been modified compared to the initial tuning of PICO, and (2) it could also be argued that the important observational target is not the ice-shelf average but the average in PICO’s box 1 (near grounding line). In view of Reese et al. (2018b), this is what matters the most for buttressing, isn’t it?

Thanks for this point. We agree that the melting in PICO’s first box should be added as a tuning parameter in future work. We changed and extended this discussion in lines 288f.

Section 4.2: The sensitivity used in LARMIP (7 to 16 m/yr/K) was estimated from plume models (Jenkins 1991 and Payne et al. 2007). It is discussed in the manuscript as if these were well-established values. These numbers may be acceptable, but there have been a few observational and more complex modelling studies since then, which have estimated sensitivities to ocean warming. It would be useful to mention whether these numbers can

still be considered as plausible (Jenkins et al., 2018; Naughten et al., 2018; Seroussi et al., 2017).

We estimate the sensitivity from the coupled experiments in Seroussi et al. (2017) for Thwaites glacier. The average sensitivity over the first twenty years is about $9.4\text{m a}^{-1}\text{K}^{-1}$ which is closer to the estimates used in LARMIP-2.

Naughten et al. (2018) report that relevant ocean temperatures driven by ACCESS under the RCP85 scenario increase by 1.8°C in the Amundsen Sea. We estimate that melt rates for that scenario increase between about 6 to about 25m a^{-1} , which yields an rough estimate of 3.3 to $13.9\text{m a}^{-1}\text{K}^{-1}$ (Fig. 7 of the paper). Especially for Pine Island and Thwaites glaciers ice shelves, melt rates increases are around 20m a^{-1} which corresponds to $11\text{m a}^{-1}\text{K}^{-1}$ which would be in line with the estimates used in LARMIP-2 and of (Seroussi et al., 2017). Similarly, Jenkins et al. (2018) show an estimate of how aggregate melt rates change quadratically based on observations for Dotson Ice Shelf (see Fig. 4c of the paper). If we assume an ice shelf area of $5,803\text{km}^2$ (Rignot et al., 2013), this yields a sensitivity of about 3.8 to $12\text{m a}^{-1}\text{K}^{-1}$ depending on initial temperatures. For the Filchner-Ronne Ice Shelf, Hellmer et al. (2012) observe an increase of basal melt rates from 0.2 to 4m a^{-1} for a warming of 2K which would imply a sensitivity of $1.9\text{m a}^{-1}\text{K}^{-1}$. A more thorough analysis of these studies is important for re-assessing parameters of PICO in future studies.

We tested the projection based on the NorESM1-M ocean forcing using different parameters for PICO that yield higher melt rate sensitivities. Figure 2 in this response shows that mass loss (relative to control simulations) increases substantially.

We added a dicussion of the sensitivities that we derived from (Seroussi et al., 2017) in lines 291ff.

Besides, it is possible that the ocean sensitivity depends on the ice shelf under consideration (for example because ocean heat entering a very large ice-shelf cavity will be entirely consumed, while only a part of the available heat is consumed in smaller cavities, which may be captured by PICO?). Please also discuss these aspects.

Done.

L.225-227: a similar correction has actually been applied to the Amundsen Sea in this paper.

Thanks for pointing this out - we changed the text accordingly.

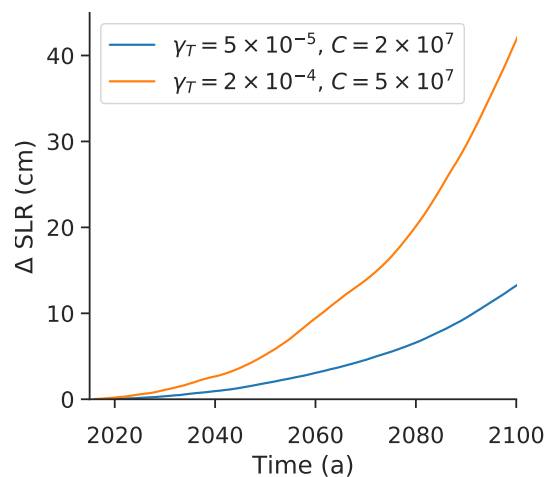


Figure 2: ISMIP6 projections for different PICO parameters. Simulations are forced with NorESM1-M ocean conditions for 2015 to 2100 similar to Figure 1b in the paper. Results are shown with respect to the control simulations. Note that control simulations show large drifts due to the parameter changes in PICO.

Anonymous referee 2

Received and published: 6 April 2020

Interactive comment on The Cryosphere Discuss., <https://doi.org/10.5194/tc-2019-330-RC2>, 2020

Summary

In The role of history and strength of the oceanic forcing in sea-level projection from Antarctica with the Parallel Ice Sheet Model, Reese et al. present the results of applying a suite of numerical experiments associated with both the ISMIP6 and LARMIP-2 model intercomparisons to the parallel ice sheet model. The key findings of this paper are that 1) the inclusion of a century-scale climate history leads to a significantly different mass loss trajectory for all of the experiments included in ISMIP6 (in particular, a climate history leads to greater mass loss), and 2) that the mechanism for parameterizing sub-shelf melting matters a lot, and that choosing between two different methods leads to an order of magnitude difference in century scale sea-level predictions.

We would like to thank the anonymous reviewer for his/her effort to review our manuscript and greatly appreciate his/her comments for improving our study.

General comments

Overall, I find the paper to be well-written and very interesting. The scientific quality is high, and the conclusions presented will be useful for those trying to hone in on areas of remaining uncertainty when prognosticating with regard to Antarctica. One overarching comment is that the experiments that are applied should be described more fully: because this paper deals with numerical experiments drawn from two other works (the main ISMIP6 forcing paper and

the LARMIP-2 paper, one of which is still in review), it would be helpful to briefly state the assumptions and differences between them (to aid in intercomparing the intercomparisons, as it were). My remaining comments are on a line-by-line basis, and may be found below.

We added a new subsection to describe the experiments and their differences in more detail, a Table S1 that contains all experiments (and the MIP's they belong to) and added more detail in the sections describing the forcing in the experiments, see, e.g., Sect. 2.2., 2.3 and 2.4. We hope that this makes it easier for the reader to understand our findings.

Specific comments

L80 A description of the mechanism for creating the ensemble, as well as the scoring method, would be appropriate here. Additionally, a discussion of the degree to which the optimal ensemble member actually matched observations would help in determining how seriously the reader should take the predictions included in this work.

We added here a detailed description of how the ensemble was created and how the initial configuration was selected in lines 87ff. The ensemble presented in the manuscript was based on a number of pre-tests of parameter influence and ranges. The ranges of PICO parameters were based on the diagnostic tuning in Reese et al. (2018). Testing for the full uncertainty related to model parameters in sea-level projections would require running the experiments on a broader ensemble.

The newly added Supplementary Figure S1 shows the scores for the ensemble. We added the state in 2015 after the historic simulation to the figure. The historic simulation score only slightly worse than the previously best run that was selected to be the initial configuration. We want to underline that given this slight difference, the final ranking depends of course on the specific choice of indicators. If, for example, present-day thinning rates would be included as suggested by Reviewer 1, we would expect the historic simulation to improve.

We added the root-mean-square deviation in ice-stream velocity and ice thickness as well as deviation in grounding line positions for both initial configurations to the manuscript in lines 104ff.

L86 Add "forcing" after "historic". Done.

L89 Please add a citation for NorESM1-M. Done.

L89-90 Please describe how the climate constants were selected for 1850-1949.

We added an explanation in lines 130ff.

L90-91 I don't understand what this 'new climatology' is. Please describe in more depth what this sentence means.

We added a detailed description in lines 137ff.

Note that the time period of the climatology (1995 – 2014) is in line with time period used for the preprocessing of data in ISMIP6.

L91 "resprective" -> "respective" **Done.**

L93 "that" -> "which" **Done.**

L97-97 The constants C and γ_T need units specified. **Done.**

L99-100 The decision to depart from observations for the Amundsen Sea due to a qualitatively undesirable model behavior merits some additional consideration. Why is lowering the temperature necessary? Does this imply that the ocean model is doing something wrong, or that the ice sheet model is doing something wrong? What are the ramifications of this, and how much faith should we have in C and γ_T under this alteration?

Thanks for bringing up this point. Please refer to the reply to the respective major and specific comments by Reviewer 1.

L107 "We here exemplify ..." is a weird sentence that can probably be removed. **Done.**

L114 The two configurations are similar in ice thickness, volume, and speed, but how about in trend? This is hinted at, but should probably be specified more explicitly.

Thanks for making this point, we added it in lines 172f.

L115-119 This whole paragraph is a bit unclear. What does "these" refer to in the third sentence? What is "drift in the initial configuration"? What is an "increase in ocean forcing"?

We rewrote the whole paragraph to make it better understandable.

L124 An increase in mass balance would typically imply a lower mass loss rate, but I don't think that's what is meant here. Try to be more explicit about the signs of the figures being reported.

We switched the signs so that basal mass balance is negative, i.e., a decrease means now higher mass loss, see line 179, Table 1 etc.

L125-126 I don't understand this sentence. How is "more realistic" defined?

We meant that present-day Antarctica is currently losing mass, hence the 'historic' initial configuration that has a tendency to lose mass is closer to observations (compared along that dimension) than the pseudo-steady state simulation that has a tendency to gain mass. We changed the text accordingly in line 182.

Table 2 I think that there is a typo here: the text says ISMIP6, but should read LARMIP-2, unless I am gravely misunderstanding something. **Done.**

L209 I would like to see a more specific description of how the step-forcing experiments mentioned here were performed and analyzed; as it stands, the reader is left to extrapolate from Fig. 6 how these numbers were derived.

We added a description of the step forcing experiments in lines 270f.

Sec. 4.3 This paragraph seems somewhat underdeveloped, given that the role of historic trajectory is one of the key points of the paper (it's in the title!). Is there a strong trend baked into each simulation? Is there a way to analyze whether the historic model hits a tipping point that the pseudo-steady model doesn't? There must be a reason behind why this difference exists.

We extended this section to discuss these hypotheses, added a new figure to the Supplementary Information showing the rates of sea-level contribution for the ISMIP6-simulations (Figure S6) and estimate the LARMIP-2 sea-level probability distribution for the pseudo-steady state configuration. The effect of the historic simulation is less pronounced in the LARMIP-2 experiments, probably because the forcing is stronger, thereby reducing effects of internal dynamics. If a tipping point has been crossed in the simulation could be estimated by performing equilibrium and hysteresis experiments, which would be very interesting for a next study.

References

- Favier, L., Durand, G., Cornford, S. L., Gudmundsson, G. H., Gagliardini, O., Gillet-Chaulet, F., Zwinger, T., Payne, A. J., and Le Brocq, a. M. (2014). Retreat of Pine Island Glacier controlled by marine ice-sheet instability. *Nature Climate Change*, 5(2):117–121.
- Hellmer, H. H., Kauker, F., Timmermann, R., Determann, J., and Rae, J. (2012). Twenty-first-century warming of a large antarctic ice-shelf cavity by a redirected coastal current. *Nature*, 485(7397):225.
- Jenkins, A., Shoosmith, D., Dutrieux, P., Jacobs, S., Kim, T. W., Lee, S. H., Ha, H. K., and Stammerjohn, S. (2018). West antarctic ice sheet retreat in the amundsen sea driven by decadal oceanic variability. *Nature Geoscience*, 11(10):733.
- Jourdain, N. C., Asay-Davis, X. S., Hattermann, T., Straneo, F., Seroussi, H., Little, C. M., and Nowicki, S. M. J. (under review). Ocean forcing for the ISMIP6 Antarctic ice sheet projections. *The Cryosphere Discuss.*, pages 1–33.
- Naughten, K. A., Meissner, K. J., Galton-Fenzi, B. K., England, M. H., Timmermann, R., and Hellmer, H. H. (2018). Future projections of antarctic ice shelf melting based on cmip5 scenarios. *Journal of Climate*, 31(13):5243–5261.
- Reese, R., Albrecht, T., Mengel, M., Asay-Davis, X., and Winkelmann, R. (2018). Antarctic sub-shelf melt rates via pico. *The Cryosphere*, 12(6):1969–1985.
- Rignot, E., Jacobs, S., Mouginot, J., and Scheuchl, B. (2013). Ice-shelf melting around Antarctica. *Science*, 341(6143):266–270.

Schmidtko, S., Heywood, K. J., Thompson, A. F., and Aoki, S. (2014). Multidecadal warming of Antarctic waters. *Science*, 346(6214):1227–1231.

Seroussi, H. et al. (under review). Ismip6-antarctica: results. *The Cryosphere*.

Seroussi, H., Nakayama, Y., Larour, E., Menemenlis, D., Morlighem, M., Rignot, E., and Khazendar, A. (2017). Continued retreat of thwaites glacier, west antarctica, controlled by bed topography and ocean circulation. *Geophysical Research Letters*.

The role of history and strength of the oceanic forcing in sea-level projections from Antarctica with the Parallel Ice Sheet Model

Ronja Reese¹, Anders Levermann^{1,2,3}, Torsten Albrecht¹, H el ene Seroussi⁴, and Ricarda Winkelmann^{1,2}

¹ Potsdam Institute for Climate Impact Research (PIK), Member of the Leibniz Association, P.O. Box 60 12 03, 14412 Potsdam, Germany

² University of Potsdam, Institute of Physics and Astronomy, Karl-Liebknecht-Str. 24-25, 14476 Potsdam, Germany

³ LDEO, Columbia University, New York, USA

⁴ Jet Propulsion Laboratory, California Institute of Technology, Pasadena, CA, USA

Correspondence: Ronja Reese (ronja.reese@pik-potsdam.de)

Abstract. Mass loss from the Antarctic Ice Sheet constitutes the largest uncertainty in projections of future sea-level rise. Ocean-driven melting underneath the floating ice shelves and subsequent acceleration of the inland ice streams is the major reason for currently observed mass loss from Antarctica and is expected to become more important in the future. Here we show that for projections of future mass loss from the Antarctic Ice Sheet, it is essential (1) to better constrain the sensitivity of sub-shelf melt rates to ocean warming, and (2) to include the historic trajectory of the ice sheet. In particular, we find that while the ice-sheet response in simulations using the Parallel Ice Sheet Model is comparable to the median response of models in three Antarctic Ice Sheet Intercomparison projects – initMIP, LARMIP-2 and ISMIP6 – conducted with a range of ice-sheet models, the projected 21st century sea-level contribution differs significantly depending on these two factors. For the highest emission scenario RCP8.5, this leads to projected ice loss ranging from 1.4 to 4.0 cm of sea-level equivalent in ~~the ISMIP6 simulations where the~~ simulations in which ISMIP6 ocean forcing drives the PICO ocean box model where parameter tuning leads to a comparably low sub-shelf melt sensitivity ~~is comparably low, and in which no surface forcing is applied. This is~~ opposed to a likely range of ~~9.2 to 35.99.1 to 35.8~~ cm using the exact same initial setup, but emulated from the LARMIP-2 experiments with a higher melt sensitivity ~~based on, even though both projects use forcing from climate models and melt rates are calibrated with previous~~ oceanographic studies. Furthermore, using two initial states, one with ~~and one without~~ a previous historic simulation from 1850 to 2014 and one starting from a steady state, we show that while differences between the ice-sheet configurations in 2015 ~~are marginal seem marginal at first sight~~, the historic simulation increases the susceptibility of the ice sheet to ocean warming, thereby increasing mass loss from 2015 to 2100 by ~~about 5 to~~ 50%. Hindcasting past ice-sheet changes with numerical models would thus provide valuable tools to better constrain projections. Our results emphasize that the uncertainty that arises from the forcing is of the same order of magnitude as the ice-dynamic response for future sea-level projections.

1 Introduction

Observations show that the Antarctic Ice Sheet is currently not in equilibrium and that its contribution to global sea-level rise is increasing (Shepherd et al., 2018). Its future contribution is the largest uncertainty in sea-level projections (Pörtner et al., 2019) with its evolution driven by snowfall increases (e.g., Ligtenberg et al., 2013; Frieler et al., 2015) that are counteracted by increased ocean forcing (e.g., Hellmer et al., 2012; Naughten et al., 2018) and potentially instabilities such as the Marine Ice Sheet Instability (Weertman, 1974; Schoof, 2007) and the Marine Ice Cliff Instability (DeConto and Pollard, 2016).

In recent years, sea-level projections of the Antarctic Ice Sheet were conducted with individual ice-sheet models (e.g., DeConto and Pollard, 2016; Golledge et al., 2019) and extended by comprehensive community efforts such as the Ice Sheet Model Inter-comparison Project for CMIP6 (ISMIP6, Nowicki et al., 2016, in prep; Seroussi et al., under review) and the Linear Antarctic Response Model Intercomparison Project (LARMIP-2, Levermann et al., 2014, 2020) projects. In ISMIP6, a protocol for Antarctic projections was developed and ice-sheet model responses to oceanic and atmospheric forcing from selected CMIP5 models (Barthel et al., 2019) were gathered and compared for the first time. As a first step of ISMIP6, initMIP-Antarctica did test the effect of different model initialisation on idealized experiments (Seroussi et al., 2019). While the response of the ice sheet to surface mass balance forcing was similar among the models, they showed very different responses to basal melt rate changes. Similarly, in ISMIP6 a large spread in model projections is found, [ranging with ice volume changes](#) from -7.8 to 30.0 cm of Sea-Level Equivalent (SLE) under the highest greenhouse gas emission scenario (Representative Concentration Pathway RCP8.5) with the largest uncertainties coming from ocean-induced melt rates, the calibration of melt rates and the ice dynamic response to oceanic changes. [The ISMIP6 projections are given with respect to control simulation, hence not considering current trends of mass loss.](#)

Sea-level estimates in ISMIP6 are in many cases substantially lower than the ocean-driven mass loss projected by LARMIP-2. In LARMIP-2, the sea-level contribution of the Antarctic Ice Sheet is emulated from step-forcing experiments using linear response function theory (Winkelmann and Levermann, 2013). A median mass loss of 1817 cm with a likely range from 9 cm to 3836 cm and a very likely range of 6 cm to 6158 cm is found. In contrast to ISMIP6, atmospheric changes, [that add between \$-2.5\$ and \$84.5\$ mm SLE depending on the CMIP5 forcing,](#) are not considered in LARMIP-2, and we here [also](#) focus on the dynamic, ocean-driven response of the ice sheet.

In projections of the future Antarctic sea-level contribution following the ISMIP6 and LARMIP-2 protocols, oceanic forcing is obtained from sub-surface ocean conditions in general circulation models, e.g., from results of the fifth phase of the Coupled Model Intercomparison Project (CMIP5, Taylor et al., 2012). This approach takes into account that sub-shelf melt rates are mainly driven by inflow of ocean water masses at depth (Jacobs et al., 1992). However, CMIP5 models do not include ice-shelf cavities and related feedbacks that might increase the future oceanic forcing on the ice shelves ([Bronse laer et al., 2018; Golledge et al., 2019](#))([Timmermann and Goeller, 2017; Donat-Magnin et al., 2017; Bronse laer et al., 2018; Golledge et al., 2019](#)). [Ocean temperatures from CMIP5 models therefore have to be extrapolated into ice-shelf cavities \(Jourdain et al., under review\)](#). Alternatively, output from [regional high-resolution](#) models that resolve ocean dynamics on the continental shelf and within the ice-shelf cavities could be used (e.g., Hellmer et al., 2012; Naughten et al., 2018).

The sub-surface ocean forcing informs ~~parameterisations~~ parameterizations that provide melt rates underneath the ice shelves for ice-sheet models. For the ISMIP6 experiments, a depth-dependent, non-local ~~parameterisation~~ parameterization and a depth-dependent, local ~~parameterisation~~ parameterization have been proposed (Jourdain et al., under review) that both mimic a quadratic dependency of melt rates on thermal forcing (Holland et al., 2008). As an alternative, more complex modules that capture the basic physical processes within ice-shelf cavities ~~haven~~ have been developed recently (Lazeroms et al., 2018; Reese et al., 2018a). We here analyse results as submitted to ISMIP6 that apply the Potsdam Ice-shelf Cavity mOdel (PICO; Reese et al., 2018a) which extends the ocean box model (Olbers and Hellmer, 2010) for application in three-dimensional ice-sheet models. The model has been tested and compared to other ~~parameterisations~~ parameterizations for an idealized geometry (Favier et al., 2019). In this case, the induced ice-sheet response matches the response driven by a three-dimensional ocean model. In contrast to ISMIP6, the LARMIP-2 experiments are forced by basal-melt rate changes directly. Scaling factors between global mean temperature changes and Antarctic sub-surface temperature changes are determined from CMIP5 models. These are used to generate ocean temperature forcing under different RCP scenarios emulated from MAGICC-6.0 RCP realisations (Meinshausen et al., 2011). Sub-shelf melt rates are assumed to increase by 7 to 16 m a⁻¹ per degree of sub-surface ocean warming, based on Jenkins (1991) and Payne et al. (2007).

Here we compare simulations with the Parallel Ice Sheet Model as submitted to ISMIP6 with results obtained following the LARMIP-2 protocol and analyse (1) the effect of the oceanic forcing and (2) the effect of a historic simulation preceding the projections. In Sect. 2 we describe the methods used and the initial configurations of PISM. This is followed by an analysis of the experiments for ISMIP6 with only ocean forcing applied and the results obtained when following the LARMIP-2 protocol in Sect. 3. These are compared and discussed in Sect. 4 and 5.

2 Methods

We use the comprehensive, thermo-mechanically coupled Parallel Ice Sheet Model (PISM, Bueler and Brown, 2009; Winkelmann et al., 2011; the PISM authors, 2019) which employs a superposition of the Shallow-Ice and Shallow-Shelf Approximations (Hutter, 1983; Morland, 1987; MacAyeal, 1989). We apply a ~~power-law for sliding~~ power-law relationship between SSA basal sliding velocities and basal shear stress with a Mohr–Coulomb criterion relating the yield stress to parameterized till material properties and the effective pressure of the overlaying ice on the saturated till (Bueler and Pelt, 2015). Basal friction and sub-shelf melting are linearly interpolated on a sub-grid scale around the grounding line (Feldmann et al., 2014). ~~The surface gradient in the driving stress~~ In order to improve the approximation of driving stress across the grounding line, the surface gradient is calculated using centered differences of the ice thickness across the grounding line. We apply eigen-calving (Levermann et al., 2012) in combination with the removal of ice that is thinner than 50 m or extends beyond present-day ice fronts (Fretwell et al., 2013).

2.1 Initial configurations

We use two model configurations of the Antarctic Ice Sheet that were submitted to ISMIP6, one with ~~and one without~~ a preceding historic simulation from 1850 to 2014 and one starting from a steady-state. Both configurations share the same initialisation procedure: Starting starting from Bedmap2 ice thickness and topography (Fretwell et al., 2013), a spin-up spin-up is run for 400,000 years with constant geometry to obtain a thermodynamic equilibrium with present-day climate on 16 km. Based on this, an ensemble of simulations ~~for varying parameters related to basal sliding is run over 12,000 years to near steady-state conditions on 8 horizontal resolution with~~ with varying model parameters is run for several thousand years towards dynamic equilibrium on 8 km horizontal resolution. The simulations employ 121 vertical layers with a quadratic spacing from 13 m at the ice shelf base to 100 m towards the surface. We vary parameters of PICO (heat exchange coefficient γ_T and overturning coefficient C) as well as the minimum till friction angle in the parameterized till material properties (Φ_{win}). The initial configuration ~~was selected from this ensemble by scoring against~~ is selected in two steps: after 5000 years of model simulation, 5 candidates that compare best to present-day observations of ice geometry and speed (Fretwell et al., 2013; Rignot et al., 2011) are selected and continued. After 12,000 years the best fit equilibrium result was selected among them and used as initial configuration for the projections, see Fig. S.1. We assess the ensemble members at each step using a scoring method (Pollard et al., 2016; Albrecht et al., 2020) that tests for root-mean-square deviation to present-day ice thickness, ice-stream velocities, as well as deviations in grounded and floating area, and the average distance to the observed grounding line position. We lay a specific focus on the Amundsen region, Filchner-Ronne and Ross ice shelves by additionally evaluating each indicator for these drainage basins individually.

The historic simulation is based on the same initial steady-state configuration and additionally applies atmospheric and oceanic forcing over the period from 1850 to ~~2015-2014~~ as described below. The initial state for the experiments without historic simulation, hereafter referred to as INIT*, and the initial configuration after the historic simulation, hereafter referred to as INIT, are shown in Fig S.2. The INIT* configuration is very close to a steady-state with ice volume change rates being 5 mm over 85 years while the INIT state is out of balance with ice volume change rates being -1.5 cm over 85 years, see Table 1. The INIT state in 2014 after the historic simulation scores very similar to the best-scoring initial configuration INIT*. For example, the root-mean square deviation in stream velocity in the Amundsen Sea region is 113 m a^{-1} for INIT (improved from 116 m a^{-1} for INIT*), in the Ross Sea 35 m a^{-1} (compared to 33 m a^{-1}), in the Weddell Sea 47 m a^{-1} (38 m a^{-1}) and in the entire domain 290 m a^{-1} (262 m a^{-1}). The root-mean square deviation in grounded ice thickness is 166 m (165 m) in the Amundsen Sea, 188 m (189 m) in the Ross Sea, 167 m (167 m) in the Weddell Sea and 250 m (250 m) for the entire continent. The mean grounding line deviation is 12 km (13 km) in the Amundsen Sea, 24 km (24 km) in the Ross Sea, 14 km (15 km) in the Weddell Sea and 17 km (17 km) in the entire domain.

2.2 ~~Surface mass balance~~Experiments

We here present experiments based on the ISMIP6, LARMIP-2 and initMIP protocols that were done for both initial configurations. A list of all experiments is given in Table S.1. The initMIP experiments employ idealized forcing designed to test the model

120 response to simplified forcing of the surface mass balance (experiment 'asmb'), and the basal mass balance (experiment
'abmb') which increase linearly for 50 years and are kept constant afterwards (Seroussi et al., 2019).
For LARMIP-2, constant step-forcing perturbations of the basal mass balance (4, 8 and 16 m a^{-1}) are applied in five Antarctic
regions (Antarctic Peninsula, East Antarctica, Ross Sea, Amundsen Sea, Weddell Sea). From the modeled sea-level response,
linear response functions are derived that can be used to emulate the model's response to arbitrary melt forcing.
The ISMIP6 protocol prescribes atmospheric and oceanic forcing from CMIP5 models. We use the forcing data provided by
125 ISMIP6 for (1) NorESM1-M for RCP8.5, (2) MIROC-ESM-CHEM for RCP8.5, (3) NorESM1-M for RCP2.6 and (4) CCSM4
for RCP8.5 (experiments 1-4 in Seroussi et al., under review). To be consistent with LARMIP-2, we here only apply the ocean
forcing in projections and keep the surface mass balance constant.
We run experiments for both initial configurations with * indicating simulations starting from the pseudo-steady state in 2015,
INIT*. The control experiments for both initial configurations employ constant climate conditions as described in the following
130 two subsections.

2.3 Atmosphere forcing

Surface mass balance and ice surface temperatures for the initial configuration without historic forcing are from RACMOv2.3p2
(1986 to 2005 averages, Van Wessem et al., 2018), remapped from 27 km resolution. The historic simulation is started from
the same conditions with historic surface mass balance and surface temperature changes following the NorESM1-M simula-
135 tion as suggested by ISMIP6 (Bentsen et al., 2013). The historic forcing from NorESM1-M is normalized to its initial period
(1950-1980) and the anomalies are then added to the constant climatology from RACMO. Since the provided data starts in
1950, surface mass balance and temperatures are constant between 1850 and 1949. ~~A new climatology for the experiments~~ Over
that period, the aggregated, yearly surface mass balance is very similar to the RACMO climatology, as shown in Fig. S.3.
In contrast to ISMIP6, where surface mass balance and surface temperature changes are driven by GCM data, we here keep
140 surface conditions - in line with LARMIP-2 - constant throughout the projections. Note that due to changes in the ice-sheet
extent, surface mass balance integrated over the entire ice sheet might change slightly, see Table 1. Surface mass balance and
temperatures in the projections that start from the pseudo steady-state INIT* are given by the RACMO climatology. For the
projections based on the historic simulation ~~is obtained from~~ we created a new climatology to account for increases in surface
mass balance and temperatures in the historic simulation. We avoid using exceptionally high or low values that arise from
145 interannual variability at a specific snapshot in time by using the 1995 to 2014 average of the ~~respective~~ respective fields.

2.4 Basal mass balance Ocean forcing

Sub-shelf melt rates are calculated by PICO ~~that~~ which extends the ocean box model by Olbers and Hellmer (2010) for ap-
plication in 3-dimensional ice sheet models (Reese et al., 2018a). It mimics the vertical overturning circulation in ice-shelf
cavities and has two model parameters that apply for all Antarctic ice shelves simultaneously: C related to the strength of the
150 overturning circulation and γ_T related to the vertical heat exchange across the ice-ocean boundary layer. We here use param-
eters ~~$C = 1e6$~~ $C = 1 \times 10^6 \text{ m}^6 \text{ s}^{-1} \text{ kg}^{-1}$ and $\gamma_T = 3 \times 10^{-5} \text{ m s}^{-1}$ that were found to yield realistic melt rates in comparison

to present-day estimates (Reese et al., 2018a; Rignot et al., 2013) ~~with~~. The value of γ_T is slightly higher than the reference value ~~as an outcome of the ensemble study, see Fig. S.1.~~

We initialize PICO with an ocean data compilation from ~~Locarnini and Smolyar (2018)~~ the World Ocean Atlas 2018 pre-release (Locarnini et al., 2018; Zweng et al., 2018) and Schmidtko et al. (2014). ~~Temperatures in the Amundsen Sea had to be reduced to cold conditions (-1.25°)~~ PICO is driven by ocean temperature and salinity averaged over the depth of the continental shelf within each drainage basin. The data from the WOA2018 pre-release is processed by determining the relevant depth from bathymetric access to ice-shelf cavities. In Dronning Maud Land (PICO basins 2 to prevent collapse of the region-5), where ocean temperatures have a warm bias due to the lack of data along narrow continental shelves, values from Schmidtko et al. (2014) were used. Using the currently observed ‘warm’ conditions in the Amundsen Sea, we found that region to collapse in the initial ensemble irrespective of basal sliding parameters. As this region is out of balance today due to oceanic forcing (e.g., Konrad et al., 2018; Sh ~~it would be inconsistent to initialize our model by running it towards equilibrium over several thousand years applying constant present-day climate forcing. We hence reduced temperatures in the Amundsen Sea to ‘cold’ conditions (-1.25°C , Jenkins et al., 2018)~~

~~ISMIP6 ocean forcing.~~

Ocean temperature and salinity forcing is calculated from CMIP5 models using an anomaly approach as suggested for ISMIP6 (Barthel et al., 2019; Jourdain et al., under review). We average these values over 400 to 800 m depth to obtain suitable input for PICO. The historic forcing is based on NorESM1-M (as suggested for ISMIP6) and ~~a anomalies are normalized to the initial period (here 1850-1900), similar to the atmosphere forcing. A~~ new ocean climatology for the initial configuration experiments starting from the historic simulation is obtained from the 1995 to 2014 average conditions. ~~The experiments are run using~~

For LARMIP-2, we add melt rate anomalies to the underlying PICO melt rates in different Antarctic regions as described in Levermann et al. (2020). Using linear response theory, the probability distribution of the sea-level contribution for RCP8.5 is then calculated following the LARMIP-2 protocol. ~~We here exemplify the procedure for the historic configuration.~~

3 Results

We ~~here present~~ present here (1) the results for the two initial configurations submitted to ISMIP6 and (2) the sea-level estimates for RCP8.5 obtained following the LARMIP-2 and ISMIP6 experiments based on the historic configuration.

3.1 Initial configurations and historic simulation

The two initial configurations for 2015, one based on a pseudo-equilibrium and one on a historic simulation from 1850 to 2014, do not differ much in terms of state variables such as ice thickness, volume or speed (see Sect. 2.1). ~~However, the configurations~~ have opposed change rates: INIT* has a small tendency to gain mass and INIT is clearly out of balance and loses mass (compare the control simulations in Table 1). Over the historic period, the ice sheet thins along its margins through increased sub-shelf melting and at the same time thickens in the interior due to more snowfall. These signals are smaller than 50 m over grounded regions, see ~~also~~ Fig. S.2. The thinning of ice shelves around the margins and subsequent reduction of buttressing causes the

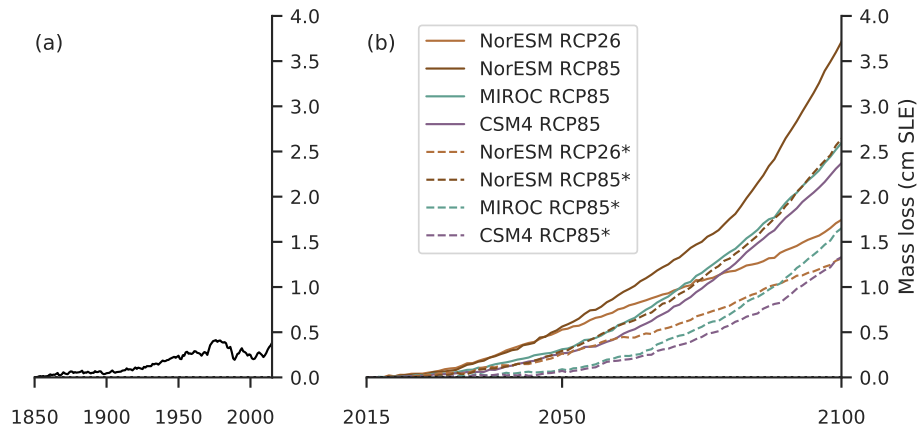


Figure 1. Mass loss-Historic simulation and projections of the Antarctic Ice Sheet driven by ISMIP6 ocean forcing between 2015 and 2100. Shown is the evolution of the volume above flotation (VAF) sea-level contribution (a) for the historic simulation relative to the start conditions its control simulation and (b) for the projections with respect to the control simulations, in cm sea-level equivalent (SLE). The historic period from 1850 to 2014 is indicated by the grey background, the projection period from 2015 to 2100 by the white background. Experiments are initialized either from a historic run (solid lines) or from the initial state (dashed lines) and forced with changes in ocean temperature and salinity from the ISMIP6 experiments no. 1 to 4 with the respective CMIP5 model indicated in the legend.

ice streams and ice shelves to slightly speed up over the historic simulation. These variations are The sensitivity of the modeled
 185 ice thickness and velocities to the historic forcing is smaller than the range due to parameter variations in the model ensemble.
In total, the ice sheet gains mass which is equivalent to 1.6 of sea-level drop over the historic period, see Table 1. This mass
gain over the historic simulation can be explained through the drift in the initial configuration which is 4.9 over 85 years (this
simulation is called ctrl* in the following) which is offset by an increasing ocean forcing sensitivity to different parameters in the
initial ensemble, see Fig. S.1. Overall, continent-wide aggregated basal mass balance decreases stronger than the aggregated
 190 surface mass balance increases, leading to mass loss of 3.6 mm SLE between 1850 and 2014 in comparison to the historic
control simulation, see Fig. 1 and Fig. S.3. Note that the pseudo-equilibrium simulation is not fully in equilibrium, but has
a small tendency to gain mass as evident from ctrl*. In contrast, the control run started from the historic simulation (ctrl)
is clearly out of equilibrium and shows a This is smaller than the observed mass loss of 14.9 between 2015 and 2100. This
change in trend is due to a net negative mass balance through the historic period with surface mass balance increased by 68^{-1}
 195 while basal mass balance increased by 420^{-1} and calving fluxes stay approximately constant. Hence total 7.6 ± 3.9 mm SLE
between 1992 and 2017 (Shepherd et al., 2018).

The patterns of present-day mass loss thickness changes (here 2014) is more realistic than starting from a are more realistic in
the historic configuration INIT than for the pseudo-equilibrium state INIT*. Furthermore, highest mass losses are simulated in
 the Amundsen Sea and Totten regions which agrees with observations (Shepherd et al., 2018). Both initial configurations are
 200 further compared to other model configurations and to present-day ice thickness and velocities in Seroussi et al. (under review).

Table 1. Mass loss and evolution of surface and basal mass balance in ISMIP6 simulations. All values, except for the ctrl simulations, are relative to the respective control simulation.

Experiments	$\Delta\text{BMB-SMB}$	$\Delta\text{SMB-BMB}$	$\Delta\text{SMB}-\Delta+\Delta\text{BMB}$	Ice mass change-Sea-level contribution
	Gta ⁻¹	Gta ⁻¹	Gta ⁻¹	mm SLE
historic <u>ctrl</u>	<u>420-3</u>	<u>68-8</u>	<u>-351-11</u>	<u>1.6-5.2</u>
<u>ctrl-historic</u>	<u>-8-65</u>	<u>-428</u>	<u>-362</u>	<u>3.6</u>
<u>ctrl</u>	-17	<u>8</u>	-9	<u>-14.9-14.9</u>
asmb	<u>21-764</u>	<u>747-28</u>	<u>726-735</u>	<u>104.4-119.3</u>
abmb	<u>531-51</u>	<u>-68-538</u>	<u>-599-590</u>	<u>-57.6-42.7</u>
NorESM RCP85	<u>1063-41</u>	<u>-58-1071</u>	<u>-1121-1112</u>	<u>-54.5-39.6</u>
MIROC RCP85	<u>740-24</u>	<u>-41-748</u>	<u>-781-772</u>	<u>-42.5-27.6</u>
NorESM RCP26	<u>99-23</u>	<u>-39-107</u>	<u>-138-130</u>	<u>-33.6-18.7</u>
CCSM4 RCP85	<u>782-31</u>	<u>-47-790</u>	<u>-829-821</u>	<u>-40.2-25.3</u>
ctrl*	<u>-19-4</u>	<u>19</u>	23	<u>4.9-4.9</u>
asmb*	<u>5-770</u>	<u>774-25</u>	<u>769-746</u>	<u>122.4-117.5</u>
abmb*	<u>543-56</u>	<u>-52-562</u>	<u>-595-618</u>	<u>-34.9-39.8</u>
NorESM RCP85*	<u>1005-40</u>	<u>-36-1024</u>	<u>-1041-1064</u>	<u>-22.2-27.1</u>
MIROC RCP85*	<u>759-30</u>	<u>-26-778</u>	<u>-785-808</u>	<u>-12.1-17.0</u>
NorESM RCP26*	<u>60-25</u>	<u>-21-79</u>	<u>-81-104</u>	<u>-8.6-13.5</u>
CCSM4 RCP85*	<u>768-28</u>	<u>-24-787</u>	<u>-792-815</u>	<u>-8.7-13.7</u>

Experiments without the historic run are indicated by *. Changes in basal and surface mass balance from the first to the last time step in the experiments (i.e., from 1850 to 2014 in the historic run and from 2015 to 2100 in the other experiments).

3.2 Comparison to initMIP Antarctica

Results from the idealized surface mass balance experiment ‘asmb’ as described in initMIP Antarctica (Seroussi et al., 2019) are very similar for both initial states with 119 mm SLE of mass gains for the ‘historic’ configuration INIT and 118 mm SLE for the ‘cold-start’ configuration INIT* after 85 years of simulation with respect to the control simulations, see Table 1. This is close to the response of the different models that participated in initMIP Antarctica which showed mass gains between 125 and 186 mm SLE after 100 years.

For the idealized basal melt rate experiment ‘abmb’ from initMIP Antarctica, both states are also quite similar with mass loss of 43 and 40 mm SLE after 85 years, respectively, see Table 1. In comparison, in Seroussi et al. (2019) a model spread of 13 to 427 mm SLE after 100 years is reported. Results for both configurations presented here are close to the median of model results for both experiments tested in initMIP Antarctica.

3.3 ISMIP6 ocean-forcing experiments

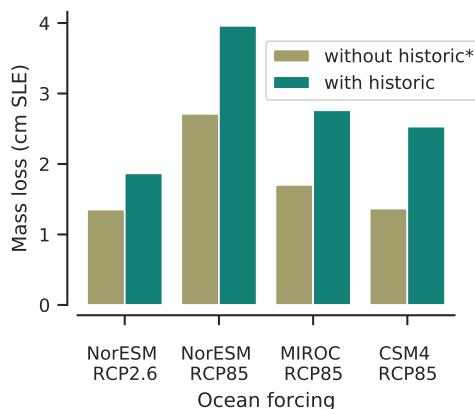


Figure 2. A preceding historic simulation increases the susceptibility of the ice sheet to ocean forcing in projections. Shown is the mass loss in simulations started directly from the initial state compared to simulations based on a historic run. The mass loss in 2100 is given with respect to the control simulation, after 85 years of applying the ocean forcing from ISMIP6 experiments no. 1 to 4 with the respective emission scenario / CMIP5 model indicated on the x-axis.

We here compare simulations for both initial configurations that are driven by ocean forcing from the ISMIP6 experiments no. 1 to 4 (Seroussi et al., under review). The sub-surface ocean changes are obtained from the CMIP5 simulations of (1) NorESM1-M for RCP8.5, (2) MIROC-ESM-CHEM for RCP8.5, (3) NorESM1-M for RCP2.6 and (4) CCSM4 for RCP8.5 (see Sect. 3.3 Seroussi et al., under review). In general, the ice sheet’s mass loss increases with stronger ocean forcing as projected for RCP8.5 in comparison to RCP2.6, see Fig. 1. The highest losses for RCP8.5 are found for NorESM1-M. The magnitude of mass loss ranges from 1.4 to 4.0 cm SLE in comparison to the control simulation, which is substantially smaller than previous estimates of Antarctica’s sea-level contribution from modelling studies (e.g., DeConto and Pollard, 2016; Golledge et al., 2011) (e.g., DeConto and Pollard, 2016; Golledge et al., 2019; Edwards et al., 2019) or expert judgement (Bamber et al., 2019). Furthermore, we find that the historic simulation makes the configuration more susceptible to ocean forcing, see Fig. 2. Ocean-driven mass loss in comparison to the control run is increased by about 50% (factor 1.5) when starting from the historic simulation in contrast to the ‘cold-start’.

3.4 LARMIP-2 basal melt rate forcing experiments

In LARMIP-2, sea-level probability distributions from the Antarctic Ice Sheet are derived using linear response functions as described in Levermann et al. (2020). The response functions are derived from experiments in which constant basal melt rate forcing is applied for five different regions of Antarctica. We here perform the same experiments for both configurations described in Sect. 2.

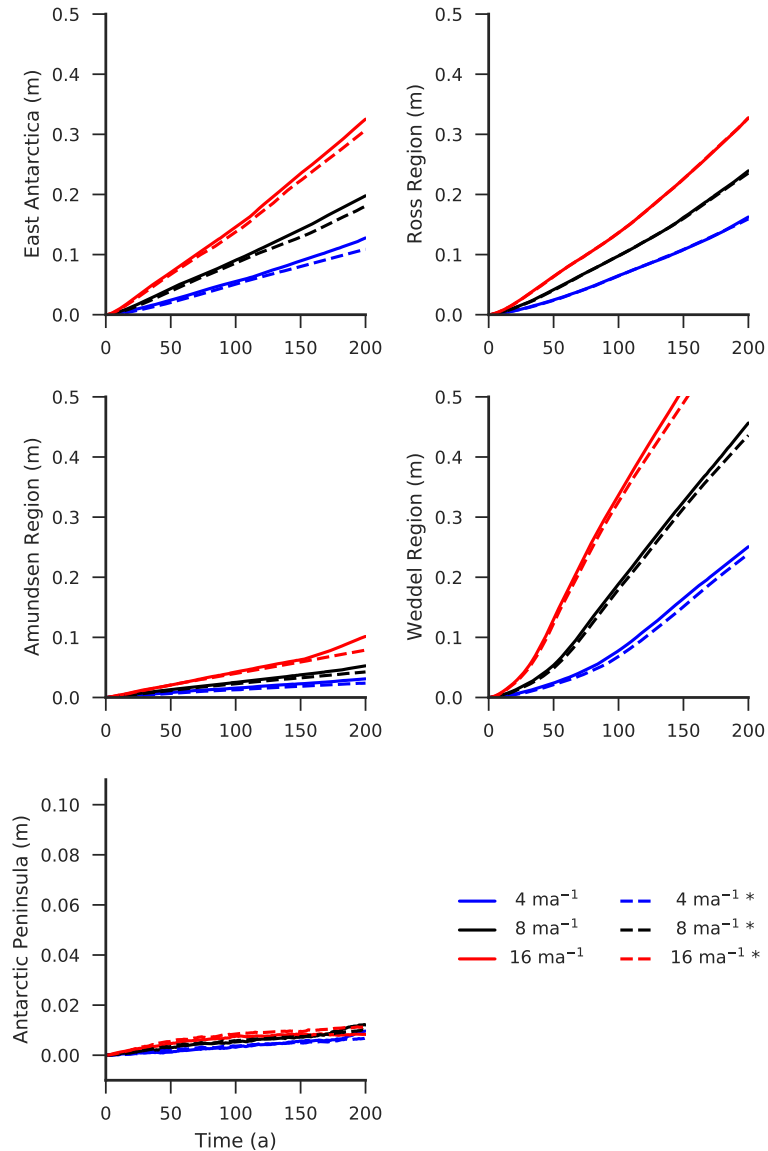


Figure 3. Mass loss of the different regions in Antarctica (indicated on y-axis) driven by constant LARMIP-2 basal melt rate forcing. For the experiments from the LARMIP-2 protocol we show the changes in volume above flotation initialized from a historic simulation (solid line) and from the initial state directly (dashed line, indicated by *). Mass loss is shown relative to the respective control simulation. From the response of the ice sheet to a constant melt rate forcing over 200 years, a response function is derived which serves then to emulate the sea-level contribution under various climate scenarios. This figure is similar to Fig. 4 in Levermann et al. (2020).

We find that for all regions the ice sheet response compares with the responses found in LARMIP-2 as, for example, in the PISM-PIK contribution that is based on a different initial state with 4 km horizontal resolution and that does not apply subgrid

Table 2. Percentiles of the probability distribution of the sea level contribution from Antarctica ~~for the ISMIP6 configuration~~ under the RCP-8.5 climate scenario (~~‘historic’ configuration~~) from 2015 to 2100, estimated following the LARMIP-2 protocol.

percentile	cm SLE (INIT*)	cm SLE (INIT)	difference (%)
5.0 %	3.4 <u>3.3</u>	<u>3.5</u>	<u>5.5</u>
16.6 %	9.2 <u>8.5</u>	<u>9.1</u>	<u>6.8</u>
50.0 %	18.4 <u>17.2</u>	<u>18.3</u>	<u>6.4</u>
83.3 %	35.9 <u>33.9</u>	<u>35.8</u>	<u>5.7</u>
95.0 %	55.1 <u>52.8</u>	<u>55.6</u>	<u>5.3</u>

230 melting, compare Fig. 3 with Fig. 4 from Levermann et al. (2020). A detailed comparison of both PISM-PIK contributions is given in Table S.2. Similar to the ISMIP6 simulations, the experiments show different responses for the two initial configurations, especially in the Weddell Sea, East Antarctica and the Amundsen Sea region. The overall difference is smaller than in the ISMIP6 experiments for the stronger forcing applied here.

Following the procedure in LARMIP-2, we derive response functions from the idealized experiments for the five Antarctic
 235 regions, ~~here exemplified for the ‘historic’ configuration.~~ We then convolve the response function with basal melt rate forcing, given in Fig. 4, to obtain a probability distribution of the future sea-level contribution for RCP8.5 which is given in Fig. 5. The ocean-driven mass loss from 2015 to 2100 has a very likely range of ~~3.4 to 55.1~~3.5 to 55.6 cm SLE, a likely range of ~~9.2 to 35.9~~9.1 to 35.8 cm SLE and a median of ~~18.4~~18.3 cm SLE (5 to 95%, 16.6 to 83.3%, and 50% percentiles, respectively, see Table 2). Similar to the ISMIP6 simulations, these results obtained for the historic initial configuration are larger than
 240 the results for the steady-state configuration, with increases between 5 and 7%. In comparison, the PISM-PIK contribution of LARMIP-2 has a very likely range of 7 to 48 cm SLE, a likely range of 11 to 31 cm SLE and a median of 19 cm SLE for the 21st century. The resulting sea-level probability distribution is hence in line with the estimates presented in LARMIP-2.

4 Discussion

In the following, we compare the results found in the ISMIP6 and LARMIP-2 experiments, discuss the role of the ocean forcing
 245 and of the historic simulation.

4.1 Comparison of LARMIP-2 and ISMIP6 sea-level projections

The projected mass loss in LARMIP-2 is an order of magnitude larger than the ocean-driven mass loss in our ISMIP6 experiments for RCP8.5, see Sect. 3. In order to understand this difference better, we here investigate the ocean forcing in more detail. ~~We thereby focus on the RCP8.5 simulation based on NorESM1-M which shows highest mass losses of all ISMIP6~~
 250 ~~experiments presented in this study.~~

Both intercomparison projects, ISMIP6 and LARMIP-2, are based on CMIP5 model sub-surface ocean temperature changes (Levermann et al., 2014; Barthel et al., 2019; Jourdain et al., under review). While they are directly applied in ISMIP6, they are

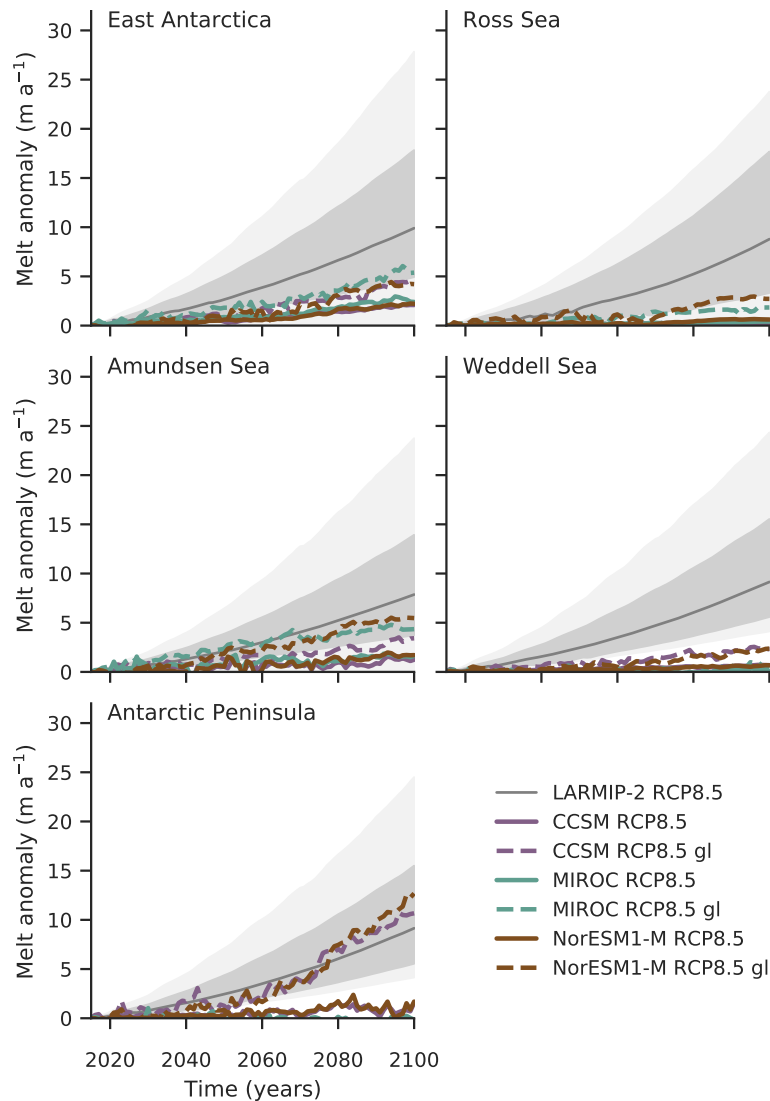


Figure 4. Projected basal melt rate changes in the different Antarctic regions from LARMIP-2 and in the ISMIP6 contribution forced with NorESM1-M, [CCSM](#) and [MIROC](#) ocean changes under RCP8.5. In LARMIP-2 spatially constant basal melt rate forcing is applied with corresponding very-likely ranges (5 to 95%-percentiles, light [red-gray](#) shading), likely ranges (66%-percentile around the median, dark [red-gray](#) shading) and median ([red-gray](#) line) for the RCP8.5 scenario. In the ISMIP6 contribution, basal melt rates are calculated by PICO, which shows higher increases close to the grounding line (PICO Box 1, [light-blue-lines](#) indicated by 'gl') than averaged over the ice shelves ([dark blue-lines](#)). Figure is similar to Fig. 3 in [Levermann et al. \(2020\)](#).

[used to derive a scaling between global mean temperatures and Antarctic sub-surface temperatures in LARMIP-2.](#) While minor differences in ocean forcing might occur due to different processing steps, a more significant difference is that the LARMIP-2 experiments are driven by basal melt rate changes emulated from the forcing, while in the ISMIP6 simulations ocean forcing

is translated into basal melt rates via sub-shelf melt ~~parameterisations~~parameterizations, in our case PICO.

Figure 4 shows projected basal melt rates and their uncertainty ranges for RCP8.5 used in LARMIP-2 together with the basal melt rate changes in the ISMIP6 ~~simulation~~simulations. Note that LARMIP-2 assumes constant changes in basal melt rates over the entire ice shelf. In contrast, since PICO mimics the vertical overturning circulation in ice-shelf cavities, basal melt rates in the ISMIP6 ~~simulation~~simulations increase strongest along the grounding line (in PICO's first box) and less towards the ice shelf front. The melt rate changes in PICO along the grounding line are hence an upper limit for the comparison to the LARMIP-2 forcing while the shelf-wide averaged changes provide a lower limit. Overall, we find that in the ISMIP6 ~~simulation~~simulations, basal-melt rates increase more in regions with smaller ice shelves than in the Ross and Weddell ~~sea~~Sea. Furthermore, we find that the basal melt rate changes in our ISMIP6 contribution in all Antarctic regions is located in the lower range (percentiles) of the LARMIP-2 forcing. Only for the Antarctic Peninsula, PICO melt rates along the grounding line increase stronger than the median in LARMIP-2 for NorESM1-M and MIROC. For all other regions, melt rate changes along the grounding line are smaller than the median in LARMIP-2 (50%-percentile). For the Amundsen Sea region, they lie within the likely range (16.6% to 83.3% percentiles), for East Antarctica and the Ross Sea, they are around the lower margin of the likely range and for the Weddell Sea, they are lower than the very likely range (5% to 95% percentiles). Shelf-wide changes are generally smaller than the likely range, for the Weddell Sea and the Antarctic Peninsula they are also smaller than the very likely range.

This is consistent with the mass loss in the ISMIP6 ~~simulation~~simulations being lower than the likely range of LARMIP-2 for almost all regions, see Fig. 5. ~~Based on the comparison of~~ These findings are underlined by the direct comparison with the PISM-PIK contribution to LARMIP-2 which is based on a different initial setup, see Sect. 3.4. Note that basal melt rate changes ~~above, we identify~~ in East Antarctica seem similar in Fig. 4 for NorESM1-M and MIROC but mass loss is higher for NorESM1-M, because the ocean forcing in the ISMIP6 simulations varies across the different ice shelves in East Antarctica. While there is stronger ocean warming in Dronning Maud Land and Amery in the MIROC forcing, the ocean warms substantially more in the Totten region for NorESM1-M. The higher vulnerability of the Totten region then causes higher overall mass loss.

In Figure 6 we assess for each region ~~two percentiles from the LARMIP-2 basal melt probability distribution: the first percentile reflects the changes along the grounding line and the second the changes~~ the mass loss by applying the response functions to the corresponding PICO melt rate changes driven by NorESM1-M ocean forcing, once averaged over the entire ice shelfshelves and once close to the grounding lines. When comparing the ~~corresponding percentiles of mass loss in LARMIP-2 (derived for the same initial configuration)~~ respective mass loss with the ISMIP6 simulation, we find that indeed the changes at the grounding line provide an upper limit while the changes over the entire ice shelf provide a lower limit for the actual mass loss. ~~No valid comparison can be made in the Weddell Sea, where the basal melt rate forcing is lower than the 0.1%-percentile from LARMIP-2, and for the shelf-wide average forcing at the Antarctic Peninsula, where mass loss is generally low. These findings are underlined by comparison with the PISM-PIK contribution to LARMIP-2 which is based on a different initial setup.~~

Overall, we find that mass losses in the ISMIP6 projections are generally lower than the likely range in LARMIP-2, and in the

290 Weddell Sea \dot{m} -losses are smaller than the very likely range, as the basal melt rate changes in the LARMIP experiments are an order of magnitude higher than those estimated with PICO and ISMIP6 forcing.

4.2 Role of ocean forcing and basal melt rate sensitivity

In order to gain a better understanding of the conversion of ocean forcing to basal melt rates in LARMIP-2 and in our ISMIP6 contribution, we further analyse the sensitivity to ocean warming.

295 We perform step-forcing experiments for both initial configurations ~~for ISMIP6~~ and diagnose the effect on basal melt rates ~~in PICO~~, see Fig. 7. Ocean temperatures are increased by 0.5, 1, 2, 3 and 4 °C and the corresponding basal melt rates for constant ice-shelf geometries are diagnosed using PICO. We find that the sensitivity in the Amundsen Sea Region is comparatively high with about $10 \text{ ma}^{-1} \text{K}^{-1}$, while the sensitivity in the Weddell Sea is lower with about $1.5 \text{ ma}^{-1} \text{K}^{-1}$, which yields for the entire Antarctic ice shelves an overall sensitivity of about $2.2 \text{ ma}^{-1} \text{K}^{-1}$. The sensitivities for melting close to the grounding line are
300 as expected a bit higher: $10.5 \text{ ma}^{-1} \text{K}^{-1}$ for the Amundsen Sea region, $3.9 \text{ ma}^{-1} \text{K}^{-1}$ for the Weddell Sea and $5.3 \text{ ma}^{-1} \text{K}^{-1}$ on average for all Antarctic ice shelves. In both cases, the Antarctic-wide sensitivity is substantially lower than the sensitivity used in LARMIP-2. In the latter study, a sensitivity between 7 and $16 \text{ ma}^{-1} \text{K}^{-1}$, based on Jenkins (1991) and Payne et al. (2007), is assumed to translate ocean forcing into sub-shelf melt rates. This is consistent with our findings in the previous section that in the ISMIP6 simulations mass loss from the Antarctic Ice Sheet, and especially from the regions that drain
305 the large Filchner-Ronne and Ross ice shelves, is smaller than the likely range estimated following the LARMIP-2 protocol. Jourdain et al. (under review) report that a different tuning of the ISMIP6 basal melt ~~parameterisation~~ parameterization to fit observations in the Amundsen Sea (from Dutrieux et al., 2014; Jenkins et al., 2018) substantially increases the sensitivity to ocean changes and ~~Seroussi et al. (2019)~~ Seroussi et al. (under review) find that this enhances the sea-level contribution by a factor of six.

310 Since the sensitivity in PICO depends on the parameters used, with the overturning coefficient C affecting the sensitivity in large ice shelves and the heat exchange coefficient γ_T affecting the sensitivity in small ice shelves, a different tuning could improve basal melt rate sensitivities and thereby lead to higher mass losses in the ISMIP6-experiments. ~~This would however affect the comparison~~ A consistency of sub-shelf melt rates ~~to~~ with present-day observations ~~, see Fig. 4 in Reese et al. (2018a)~~ One approach could be to introduce could be achieved by introducing additional degrees of freedom through temperature
315 ~~for the ice shelves~~ that reflect uncertainties in ocean properties, as for example used in Lazeroms et al. (2018) and Jourdain et al. (under review). In addition, tuning to realistic melt rates close to the grounding lines (in PICO's first box) is potentially more important than fitting shelf-wide melt rates (e.g., Goldberg et al., 2019; Reese et al., 2018b).

Few observations exist for targeted tuning of the sensitivity of basal melt rate parameterizations to ocean temperatures, hence the use of dynamic modelling of the ocean circulation in ice-shelf cavities could be explored. We estimate that the sensitivity in
320 Seroussi et al. (2017) varies between 6 and $16 \text{ ma}^{-1} \text{K}^{-1}$ with an average of $9.4 \text{ ma}^{-1} \text{K}^{-1}$ over the first twenty years of model simulation, which would be in line with the sensitivities used in LARMIP-2, see Fig. S.5.

Note that we ~~provided~~ provide linear estimates of the sensitivity of PICO in the discussion above, while Holland et al. (2008) report a quadratic dependency of melt rates on thermal forcing. They also discuss that the sensitivity depends on ice shelf cavity

properties such as the slope of the ice-shelf draft and shape of the ice shelf and that sensitivities are generally higher close to
325 the grounding line. Further factors that influence ocean circulation, such as bathymetry, also affect the ocean sensitivity. While PICO takes into account, that not all heat content of the ocean water masses that enter the cavity might be used for melting, it does not capture three-dimensional circulations in ice-shelf cavities that play a role especially for larger ice shelves such as Filchner-Ronne.

4.3 Role of historic trajectory of the Antarctic Ice Sheet

330 We find that while the historic simulation has no large effect on the initial sea-level volume (the overall difference being ~~1.61.6~~ mm SLE), it **strongly** affects the mass loss in the projections. ~~One reason might be that the initial state switches from close-to-steady state to a state that is out of balance with a tendency to mass loss . Also, the~~ A number of reasons might cause the simulations starting from the historic configuration (INIT) to be more vulnerable to ocean forcing: both simulations have different initial trends of the sea-level relevant volume and rates of ice thickness change. These trends, or the different
335 geometry after the historic simulation, might make the configuration more susceptible to ocean forcing, for example through non-linear changes in ice-shelf buttressing. In addition, the historic simulation might have pushed the ice sheet (closer) to a local instability that evolves in the projections. Figure S.6 shows the mass loss rates for all simulations presented in Sect. 3.3. In general, the rates are higher in the simulations based on the historic configuration, and these differences increase over time. In the RCP8.5 simulation forced with NorESM1-M ocean conditions, at around year 2075 a clear shift to substantially higher
340 differences is visible. We hypothesize that this could be linked to a local instability that is kicked-off for the simulations starting from the historic configuration but not for those starting from the pseudo steady state. This is less pronounced for CCSM4 and MIROC, maybe due to differences in the ocean forcing and regions contributing to sea level rise. In the idealized experiments for LARMIP-2 (Fig. 3), differences in simulations starting from the two initial states arise especially in East Antarctica, the Weddell Sea and the Amundsen Sea, less in the Ross Sea. The effect of the historic simulation is reduced for the stronger basal
345 melt rate forcing applied in the LARMIP-2 experiments, with mass loss increases in the projections between 5 and 7%. Furthermore, the ice sheet's response might have changed after the historic simulation due to changes in boundary conditions. Moreover, changes in the ice-sheet state could result since, for instance, the underlying equation system depends non-linearly on the three-dimensional temperature field. The grounding line retreats during the historic simulation slightly into deeper regions, where the local freezing point at the ice shelf base near the grounding line is decreased due to its pressure dependence. Hence
350 more heat is available for melting the ice-shelf base, which shows also in an increased sensitivity to ocean changes, see Fig. 7. In particular for lower temperatures, PICO shows a non-linear sensitivity of melt rates to ocean temperatures, as discussed in Reese et al. (2018a). Further investigations would be required to disentangle the reasons for the increased susceptibility to ocean warming after the historic simulation, also considering the strength of the forcing applied.
The sea-level contribution over the historic period from 1850 to 2014 is 3.6 mm in comparison to the control simulation. This
355 is smaller than the reported mass loss of the Antarctic Ice Sheet that amounts to 7.6 ± 3.0 mm SLE between 1992 and 2017 (Shepherd et al., 2018). An improved understanding of the basal melt rate sensitivity, potential biases in the atmospheric or

oceanic forcing, as well as an extension of the scoring with observed patterns of thickness changes would allow for performing 'hindcasting' experiments that, in a next step, could inform future projections.

5 Conclusions

360 In this study we compare sea-level projections for RCP8.5 from the Antarctic Ice Sheet as submitted to ISMIP6, using the PICO basal melt rate parameterization and constant surface mass balance forcing, and projections derived following the LARMIP-2 protocol that scales global temperatures to subsurface temperatures and melt rates, both using the Parallel Ice Sheet Model. Overall, we find that the sea-level contribution driven by ocean forcing in ISMIP6 is smaller than the likely range of the sea-level probability distribution in LARMIP-2. This difference can be explained by the comparably low sensitivity of melt rates to ocean temperature changes for the parameter tuning in ~~the basal-melt rate module PICO as used for the ISMIP6 simulations here.~~ PICO in comparison to LARMIP-2 where a sensitivity of 9 to 16m/a/K is used that we found to be consistent with a coupled simulation of Thwaites glacier (Seroussi et al., 2017). Future sea-level projections should hence carefully consider the sensitivity of basal melt rates to ocean changes. ~~Further observations~~ Additional observations of ocean conditions and ocean-induced melt rates in combination with ocean modelling are needed to better constrain this sensitivity for the diverse ice-shelf cavities in Antarctica. Furthermore, we find that while ~~including the historic evolution starting in the initial state resulting from a historic simulation from 1850 has very little effect on the simulated current ice mass or geometry, it to 2014 is virtually indistinguishable from a steady-state simulation, the historic simulation~~ increases the projected mass loss in 2100 by ~~about up to~~ 50%. This means that not only the currently committed sea-level contribution should be considered in projections, but also the effect of the historic forcing on the ice sheet's susceptibility to ocean changes. 'Hindcasting' experiments, that reproduce observed thinning rates and ice loss over the past decades, would be valuable to better constrain model parameters and improve confidence in projections. Hence, further investigations are needed to assess the sensitivity of basal melting to ocean temperatures for basal-melt parameterizations and the role of ~~historic forcing~~ historical forcing and initial conditions in future sea-level projections.

375

Code and data availability. Data and code is available from the authors upon request. Model outputs from the simulations for ISMIP6 described in this paper will be made available via the ISMIP6 project with digital object identifier. The PISM code as well as the scripts to analyse the simulations and create the figures will be made available with digital object identifier reference. The processing of the World Ocean Atlas pre-release data is described in the Bachelor thesis by Lena Nicola (2019) and shared upon request.

380

Competing interests. Helene Seroussi is an editor of the special issue The Ice Sheet Model Intercomparison Project for CMIP6 (ISMIP6). The authors declare that no other competing interests are present.

385 *Acknowledgements.* We thank the Climate and Cryosphere (CliC) effort, which provided support for ISMIP6 through sponsoring of work-
shops, hosting the ISMIP6 website and wiki, and promoted ISMIP6. We acknowledge the World Climate Research Programme, which,
through its Working Group on Coupled Modelling, coordinated and promoted CMIP5. We thank the climate modeling groups for producing
and making available their model output, the Earth System Grid Federation (ESGF) for archiving the CMIP data and providing access,
the University at Buffalo for ISMIP6 data distribution and upload, and the multiple funding agencies who support CMIP5 and ESGF. We
390 thank the ISMIP6 steering committee, the ISMIP6 model selection group and ISMIP6 dataset preparation group for their continuous en-
gagement in defining ISMIP6. This is ISMIP6 contribution No X. Development of PISM is supported by NASA grant NNX17AG65G and
NSF grants PLR-1603799 and PLR-1644277. The authors gratefully acknowledge the European Regional Development Fund (ERDF), the
German Federal Ministry of Education and Research and the Land Brandenburg for supporting this project by providing resources on the
high performance computer system at the Potsdam Institute for Climate Impact Research. Computer resources for this project have been also
395 provided by the Gauss Centre for Supercomputing/Leibniz Supercomputing Centre (www.lrz.de) under Project-ID pr94ga and pn69ru. R.R.
is supported by the Deutsche Forschungsgemeinschaft (DFG) by grant WI4556/3-1 [and through the TipACCs project that receives funding
from the European Union's Horizon 2020 research and innovation programme under grant agreement no. 820575](#). T.A. is supported by the
Deutsche Forschungsgemeinschaft (DFG) in the framework of the priority program “Antarctic Research with comparative investigations in
Arctic ice areas” by grant WI4556/2-1 and WI4556/4-1 [and in the framework of the PalMod project \(FKZ: 01LP1925D\), supported by the
400 German Federal Ministry of Education and Research \(BMBF\) as a Research for Sustainability initiative \(FONA\)](#). H.S. was supported by
grants from NASA Cryospheric Science and Modeling, Analysis, Predictions Programs.

References

- Albrecht, T., Winkelmann, R., and Levermann, A.: Glacial-cycle simulations of the Antarctic Ice Sheet with the Parallel Ice Sheet Model (PISM)—Part 2: Parameter ensemble analysis., *Cryosphere*, 14, 2020.
- 405 Bamber, J. L., Oppenheimer, M., Kopp, R. E., Aspinall, W. P., and Cooke, R. M.: Ice sheet contributions to future sea-level rise from structured expert judgment, *Proceedings of the National Academy of Sciences*, 116, 11 195–11 200, 2019.
- Barthel, A., Agosta, C., Little, C. M., Hatterman, T., Jourdain, N. C., Goelzer, H., Nowicki, S., Seroussi, H., Straneo, F., and Bracegirdle, T. J.: CMIP5 model selection for ISMIP6 ice sheet model forcing: Greenland and Antarctica, *The Cryosphere Discuss.*, <https://doi.org/10.5194/tc-2019-191>, 2019.
- 410 Bentsen, M., Bethke, I., Debernard, J. B., Iversen, T., Kirkevåg, A., Seland, Ø., Drange, H., Roelandt, C., Seierstad, I. A., Hoose, C., et al.: The Norwegian earth system model, NorESM1-M—Part 1: Description and basic evaluation of the physical climate, *Geosci. Model Dev*, 6, 687–720, 2013.
- Bronselaer, B., Winton, M., Griffies, S. M., Hurlin, W. J., Rodgers, K. B., Sergienko, O. V., Stouffer, R. J., and Russell, J. L.: Change in future climate due to Antarctic meltwater, *Nature*, 564, 53, 2018.
- 415 Bueler, E. and Brown, J.: Shallow shelf approximation as a “sliding law” in a thermomechanically coupled ice sheet model, *Journal of Geophysical Research*, 114, <https://doi.org/10.1029/2008JF001179>, 2009.
- Bueller, E. and Pelt, W. v.: Mass-conserving subglacial hydrology in the Parallel Ice Sheet Model version 0.6, *Geoscientific Model Development*, 8, 1613–1635, 2015.
- DeConto, R. M. and Pollard, D.: Contribution of Antarctica to past and future sea-level rise, *Nature*, 531, 591, 2016.
- 420 Donat-Magnin, M., Jourdain, N. C., Spence, P., Le Sommer, J., Gallée, H., and Durand, G.: Ice-Shelf Melt Response to Changing Winds and Glacier Dynamics in the Amundsen Sea Sector, Antarctica, *Journal of Geophysical Research: Oceans*, 122, 10 206–10 224, 2017.
- Dutrieux, P., De Rydt, J., Jenkins, A., Holland, P. R., Ha, H. K., Lee, S. H., Steig, E. J., Ding, Q., Abrahamsen, E. P., and Schröder, M.: Strong sensitivity of Pine Island ice-shelf melting to climatic variability, *Science*, 343, 174–178, 2014.
- Edwards, T. L., Brandon, M. A., Durand, G., Edwards, N. R., Golledge, N. R., Holden, P. B., Nias, I. J., Payne, A. J., Ritz, C., and Wernecke, 425 A.: Revisiting Antarctic ice loss due to marine ice-cliff instability, *Nature*, 566, 58–64, 2019.
- Favier, L., Jourdain, N. C., Jenkins, A., Merino, N., Durand, G., Gagliardini, O., Gillet-Chaulet, F., and Mathiot, P.: Assessment of sub-shelf melting parameterisations using the ocean–ice-sheet coupled model NEMO (v3. 6)–Elmer/Ice (v8. 3), *Geoscientific Model Development*, 12, 2255–2283, 2019.
- Feldmann, J., Albrecht, T., Khroulev, C., Pattyn, F., and Levermann, A.: Resolution-dependent performance of grounding line motion in 430 a shallow model compared with a full-Stokes model according to the MISIP3d intercomparison, *Journal of Glaciology*, 60, 353–360, <https://doi.org/doi:10.3189/2014JG13J093>, 2014.
- Fretwell, P., Pritchard, H. D., Vaughan, D. G., Bamber, J. L., Barrand, N. E., Bell, R., Bianchi, C., Bingham, R. G., Blankenship, D. D., Casassa, G., Catania, G., Callens, D., Conway, H., Cook, A. J., Corr, H. F. J., Damaske, D., Damm, V., Ferraccioli, F., Forsberg, R., Fujita, S., Gim, Y., Gogineni, P., Griggs, J. A., Hindmarsh, R. C. A., Holmlund, P., Holt, J. W., Jacobel, R. W., Jenkins, A., Jokat, W., Jordan, 435 T., King, E. C., Kohler, J., Krabill, W., Riger-Kusk, M., Langley, K. A., Leitchenkov, G., Leuschen, C., Luyendyk, B. P., Matsuoka, K., Mouginot, J., Nitsche, F. O., Nogi, Y., Nost, O. A., Popov, S. V., Rignot, E., Rippin, D. M., Rivera, A., Roberts, J., Ross, N., Siegert, M. J., Smith, A. M., Steinhage, D., Studinger, M., Sun, B., Tinto, B. K., Welch, B. C., Wilson, D., Young, D. A., Xiangbin, C., and Zirizzotti,

- A.: Bedmap2: improved ice bed, surface and thickness datasets for Antarctica, *The Cryosphere*, 7, 375–393, <https://doi.org/10.5194/tc-7-375-2013>, 2013.
- 440 Frieler, K., Clark, P. U., He, F., Buizert, C., Reese, R., Ligtenberg, S. R., Van Den Broeke, M. R., Winkelmann, R., and Levermann, A.: Consistent evidence of increasing Antarctic accumulation with warming, *Nature Climate Change*, 5, 348, 2015.
- Goldberg, D., Gourmelen, N., Kimura, S., Millan, R., and Snow, K.: How accurately should we model ice shelf melt rates?, *Geophysical Research Letters*, 46, 189–199, 2019.
- Golledge, N. R., Keller, E. D., Gomez, N., Naughten, K. A., Bernales, J., Trusel, L. D., and Edwards, T. L.: Global environmental conse-
445 quences of twenty-first-century ice-sheet melt, *Nature*, 566, 65, 2019.
- Hellmer, H. H., Kauker, F., Timmermann, R., Determann, J., and Rae, J.: Twenty-first-century warming of a large Antarctic ice-shelf cavity by a redirected coastal current, *Nature*, 485, 225, 2012.
- Holland, P. R., Jenkins, A., and Holland, D. M.: The Response of Ice Shelf Basal Melting to Variations in Ocean Temperature, *Journal of Climate*, 21, 2558–2572, <https://doi.org/10.1175/2007JCLI1909.1>, 2008.
- 450 Hutter, K. E.: *Theoretical Glaciology; Material Science of Ice and the Mechanics of Glaciers and Ice Sheets*, 1983.
- Jacobs, S., Hellmer, H., Doake, C. S. M., Jenkins, A., and Frolich, R. M.: Melting of ice shelves and the mass balance of Antarctica, *Journal of Glaciology*, 38, 375–387, <https://doi.org/10.3189/S0022143000002252>, 1992.
- Jenkins, A.: Ice shelf basal melting: Implications of a simple mathematical model, *Filchner-Ronne Ice Shelf Programme Report*, 5, 32–36, 1991.
- 455 Jenkins, A., Shoosmith, D., Dutriex, P., Jacobs, S., Kim, T. W., Lee, S. H., Ha, H. K., and Stammerjohn, S.: West Antarctic Ice Sheet retreat in the Amundsen Sea driven by decadal oceanic variability, *Nature Geoscience*, 11, 733, 2018.
- Jourdain, N. C., Asay-Davis, X. S., Hattermann, T., Straneo, F., Seroussi, H., Little, C. M., and Nowicki, S. M. J.: Ocean forcing for the ISMIP6 Antarctic ice sheet projections, *The Cryosphere Discuss.*, pp. 1–33, <https://doi.org/10.5194/tc-2019-277>, under review.
- Konrad, H., Shepherd, A., Gilbert, L., Hogg, A. E., McMillan, M., Muir, A., and Slater, T.: Net retreat of Antarctic glacier grounding lines,
460 *Nature Geoscience*, 11, 258–262, 2018.
- Lazeroms, W. M. J., Jenkins, A., Gudmundsson, G. H., and van de Wal, R. S. W.: Modelling present-day basal melt rates for Antarctic ice shelves using a parametrization of buoyant meltwater plumes, *The Cryosphere*, 12, 49–70, <https://doi.org/10.5194/tc-12-49-2018>, <https://www.the-cryosphere.net/12/49/2018/>, 2018.
- Levermann, A., Albrecht, T., Winkelmann, R., Martin, M. A., Haseloff, M., and Joughin, I.: Kinematic first-order calving law implies
465 potential for abrupt ice-shelf retreat, *The Cryosphere*, 6, 273–286, 2012.
- Levermann, A., Winkelmann, R., Nowicki, S., Fastook, J. L., Frieler, K., Greve, R., Hellmer, H. H., Martin, M. A., Meinshausen, M., Mengel, M., Payne, A. J. J., Pollard, D., Sato, T., Timmermann, R., Wang, W. L. L., and Bindschadler, R. A. A.: Projecting Antarctic ice discharge using response functions from SeaRISE ice-sheet models, *Earth System Dynamics*, 5, 271–293, 2014.
- Levermann, A., Winkelmann, R., Albrecht, T., Goelzer, H., Golledge, N. R., Greve, R., Huybrechts, P., Jordan, J., Leguy, G., Martin, D.,
470 et al.: Projecting Antarctica’s contribution to future sea level rise from basal ice shelf melt using linear response functions of 16 ice sheet models (LARMIP-2), *Earth System Dynamics*, 11, 35–76, 2020.
- Ligtenberg, S., Van de Berg, W., Van den Broeke, M., Rae, J., and Van Meijgaard, E.: Future surface mass balance of the Antarctic ice sheet and its influence on sea level change, simulated by a regional atmospheric climate model, *Climate dynamics*, 41, 867–884, 2013.
- Locarnini, R. A., A. V. M. O. K. B. T. P. B. M. M. Z. H. E. G. J. R. R. D. S. K. W. C. R. P. and Smolyar, I.: *World Ocean Atlas 2018, Volume*
475 *1: Temperature.*, <https://www.nodc.noaa.gov/OC5/woa18/woa18data.html>, nOAA Atlas NESDIS in preparation, 2018.

- Locarnini, R. A., Mishonov, A. V., Baranova, O. K., Boyer, T. P., Zweng, M. M., Garcia, H. E., Reagan, J. R., Seidov, D., Weathers, K., Paver, C. R., and Smolyar, I.: World Ocean Atlas 2018, Volume 1: Temperature, NOAA Atlas NESDIS (Vol. 81), 2018.
- MacAyeal, D. R.: Large-scale ice flow over a viscous basal sediment: Theory and application to ice stream B, Antarctica, *Journal of Geophysical Research: Solid Earth*, 94, 4071–4087, 1989.
- 480 Meinshausen, M., Raper, S. C., and Wigley, T. M.: Emulating coupled atmosphere-ocean and carbon cycle models with a simpler model, *MAGICC6–Part 1: Model description and calibration*, *Atmospheric Chemistry and Physics*, 11, 1417–1456, 2011.
- Morland, L. W.: Unconfined Ice-Shelf Flow, pp. 99–116, Springer Netherlands, Dordrecht, https://doi.org/10.1007/978-94-009-3745-1_6, 1987.
- Naughten, K. A., Meissner, K. J., Galton-Fenzi, B. K., England, M. H., Timmermann, R., and Hellmer, H. H.: Future projections of Antarctic
485 ice shelf melting based on CMIP5 scenarios, *Journal of Climate*, 31, 5243–5261, 2018.
- Nowicki, S. et al.: ISMIP6-Protocol paper, *The Cryosphere*, in prep.
- Nowicki, S. M. J., Payne, A., Larour, E., Seroussi, H., Goelzer, H., Lipscomb, W., Gregory, J., Abe-Ouchi, A., and Shepherd, A.: Ice Sheet Model Intercomparison Project (ISMIP6) contribution to CMIP6, *Geoscientific Model Development*, 9, 4521–4545, <https://doi.org/10.5194/gmd-9-4521-2016>, 2016.
- 490 Olbers, D. and Hellmer, H.: A box model of circulation and melting in ice shelf caverns, *Ocean Dynamics*, 60, 141–153, <https://doi.org/10.1007/s10236-009-0252-z>, 2010.
- Payne, A. J., Holland, P. R., Shepherd, A. P., Rutt, I. C., Jenkins, A., and Joughin, I.: Numerical modeling of ocean-ice interactions under Pine Island Bay’s ice shelf, *Journal of Geophysical Research: Oceans*, 112, <https://doi.org/10.1029/2006JC003733>, c10019, 2007.
- Pollard, D., Chang, W., Haran, M., Applegate, P., and DeConto, R.: Large ensemble modeling of the last deglacial retreat of the West
495 Antarctic Ice Sheet: comparison of simple and advanced statistical techniques, 2016.
- Pörtner, H.-O., Roberts, D., Masson-Delmotte, V., Zhai, P., Tignor, M., Poloczanska, E., Mintenbeck, K., Nicolai, M., Okem, A., Petzold, J., Rama, B., and Weyer, N. e.: IPCC, 2019: Summary for Policymakers. In: *IPCC Special Report on the Ocean and Cryosphere in a Changing Climate*, 2019.
- Reese, R., Albrecht, T., Mengel, M., Asay-Davis, X., and Winkelmann, R.: Antarctic sub-shelf melt rates via PICO, *The Cryosphere*, 12,
500 1969–1985, 2018a.
- Reese, R., Gudmundsson, G. H., Levermann, A., and Winkelmann, R.: The far reach of ice-shelf thinning in Antarctica, *Nature Climate Change*, 8, 53–57, 2018b.
- Rignot, E., Mouginot, J., and Scheuchl, B.: Ice flow of the Antarctic ice sheet, *Science*, 333, 1427–1430, 2011.
- Rignot, E., Jacobs, S., Mouginot, J., and Scheuchl, B.: Ice-shelf melting around Antarctica., *Science*, 341, 266–270,
505 <https://doi.org/10.1126/science.1235798>, 2013.
- Schmidtko, S., Heywood, K. J., Thompson, A. F., and Aoki, S.: Multidecadal warming of Antarctic waters, *Science*, 346, 1227–1231, <https://doi.org/10.1126/science.1256117>, 2014.
- Schoof, C.: Marine ice-sheet dynamics. Part 1. The case of rapid sliding, *Journal of Fluid Mechanics*, 573, 27–55, 2007.
- Seroussi, H., Nakayama, Y., Larour, E., Menemenlis, D., Morlighem, M., Rignot, E., and Khazendar, A.: Continued retreat
510 of Thwaites Glacier, West Antarctica, controlled by bed topography and ocean circulation, *Geophysical Research Letters*, <https://doi.org/10.1002/2017GL072910>, 2017.
- Seroussi, H., Nowicki, S., Simon, E., Abe-Ouchi, A., Albrecht, T., Brondex, J., Cornford, S., Dumas, C., Gillet-Chaulet, F., Goelzer, H., et al.: initMIP-Antarctica: an ice sheet model initialization experiment of ISMIP6, *The Cryosphere*, 13, 1441–1471, 2019.

- Seroussi, H. et al.: ISMIP6-Antarctica: results, *The Cryosphere*, under review.
- 515 Shepherd, A., Ivins, E., Rignot, E., Smith, B., Van Den Broeke, M., Velicogna, I., Whitehouse, P., Briggs, K., Joughin, I., Krinner, G., et al.:
Mass balance of the Antarctic Ice Sheet from 1992 to 2017, *Nature*, 558, 219–222, 2018.
- Taylor, K. E., Stouffer, R. J., and Meehl, G. A.: An Overview of CMIP5 and the Experiment Design, *Bulletin of the American Meteorological
Society*, 93, 485–498, <https://doi.org/10.1175/BAMS-D-11-00094.1>, 2012.
- the PISM authors: PISM, a Parallel Ice Sheet Model, <http://www.pism-docs.org>, 2019.
- 520 Timmermann, R. and Goeller, S.: Response to Filchner–Ronne Ice Shelf cavity warming in a coupled ocean–ice sheet model–Part 1: The
ocean perspective, *Ocean Science*, 13, 765–776, 2017.
- Van Wessem, J. M., Jan Van De Berg, W., Noël, B. P., Van Meijgaard, E., Amory, C., Birnbaum, G., Jakobs, C. L., Krüger, K., Lenaerts, J.,
Lhermitte, S., et al.: Modelling the climate and surface mass balance of polar ice sheets using RACMO2: Part 2: Antarctica (1979–2016),
Cryosphere, 12, 1479–1498, 2018.
- 525 Weertman, J.: Stability of the junction of an ice sheet and an ice shelf, *Journal of Glaciology*, 13, 3–11, 1974.
- Winkelmann, R. and Levermann, A.: Linear response functions to project contributions to future sea level, *Climate dynamics*, 40, 2579–2588,
2013.
- Winkelmann, R., Martin, M. A., Haseloff, M., Albrecht, T., Bueller, E., Khroulev, C., and Levermann, A.: The Potsdam Parallel Ice Sheet
Model (PISM-PIK) – Part 1: Model description, *The Cryosphere*, 5, 715–726, <https://doi.org/10.5194/tc-5-715-2011>, 2011.
- 530 Zweng, M. M., Reagan, J. R., Seidov, D., Boyer, T. P., Locarnini, R. A., Garcia, H. E., Mishonov, A. V., Baranova, O. K., Weathers, K.,
Paver, C. R., and Smolyar, I.: *World Ocean Atlas 2018, Volume 2: Salinity*, NOAA Atlas NESDIS (Vol. 81), 2018.

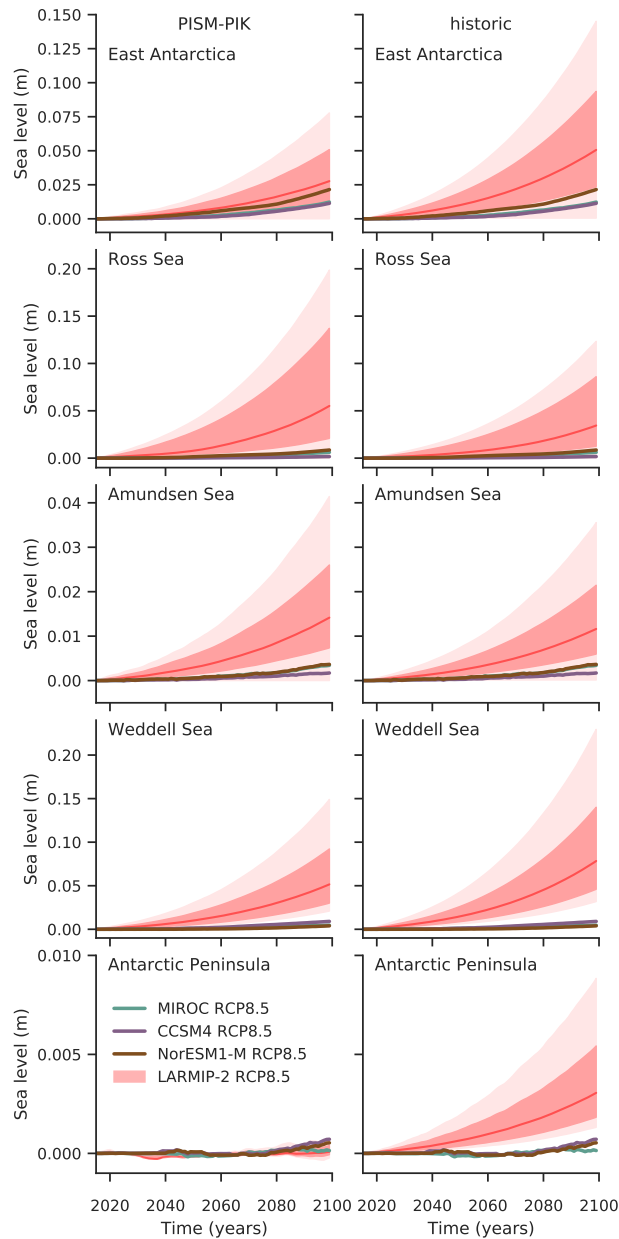


Figure 5. Projections of Antarctica’s sea level contribution under the RCP8.5 climate scenario for the different Antarctic regions for LARMIP-2 and for the ISMIP6 ~~experiment-experiments~~ driven by NorESM1-M, ~~MIROC and CCSM4~~ ocean ~~changes~~forcing. The very likely ranges (5 to 95%-percentiles, light red shading), likely ranges (16.6 to 83.3%-percentiles, dark red shading) and the respective median (50%-percentile, red lines) of mass loss is shown for (left panels) the PISM-PIK simulations submitted to LARMIP-2 and, for comparison, (right panels) estimated following LARMIP-2 for the setup as submitted to ISMIP6. ~~The sea-level-contribution-in-ISMIP6 (black-curve) is compared to percentiles of LARMIP-2 results which have consistent basal melt rate changes in the corresponding region close to the grounding line (light blue) or averaged over the ice shelves (dark blue line), see also Fig. 4. Corresponding percentiles are indicated in the left panels-~~

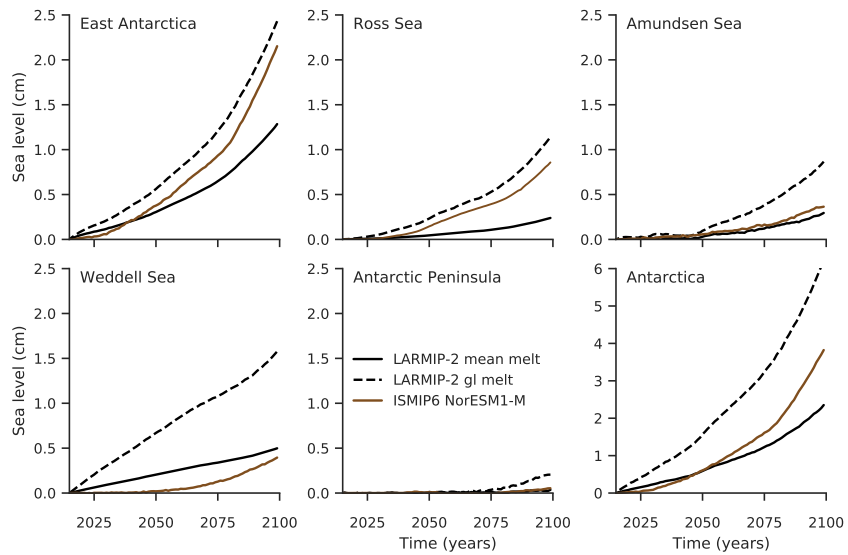


Figure 6. Projections using PICO forced with NorESM1-M ocean conditions compared to projection obtained by the response function. The response function is derived for the INIT configuration. It is applied to the basal melt rate forcing from PICO using average conditions underneath the shelves in the corresponding sector (generally an underestimation) and using the melting at the grounding line (generally an overestimation) from Fig. 4.

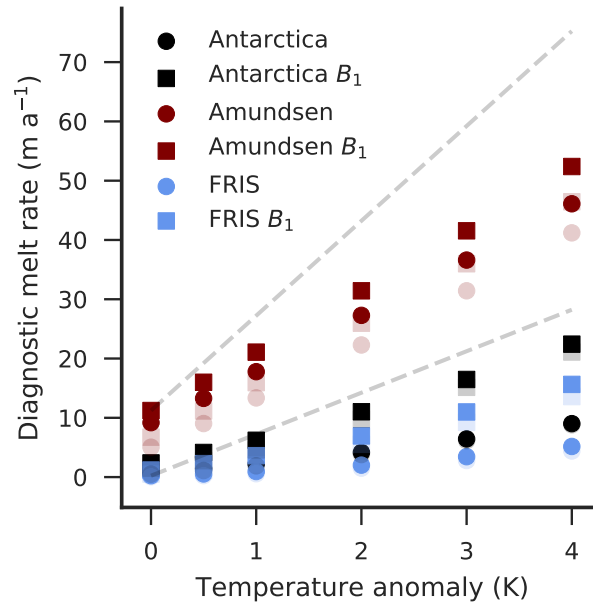


Figure 7. Sensitivity of basal melt rates to ocean temperatures in PICO. Diagnosed from the historic configuration ([solidopaque](#)) and the cold-start configuration ([shadedtransparent](#)) in 2015 using step-wise ocean temperature increases. Dots show shelf-wide averages while boxes indicate the basal melt rates close to the grounding lines (in PICO box B_1). The dashed grey lines indicate the sensitivity estimates used in Levermann et al. (2020).

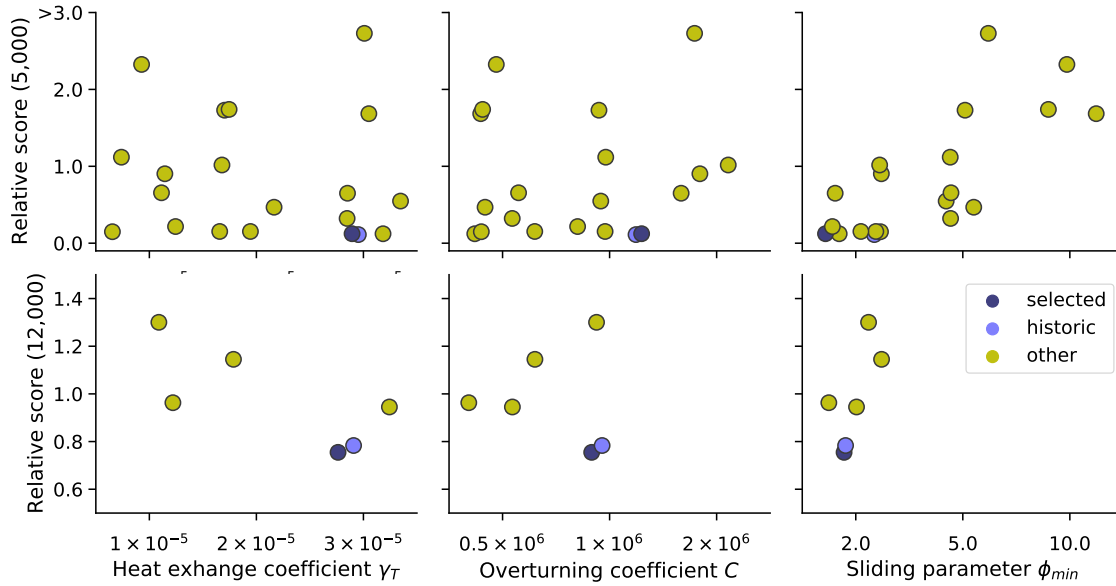


Figure S.1. Comparison of PISM ensemble members with present-day geometry and velocities (Fretwell et al., 2013; Rignot et al., 2011) after (upper row) 5,000 and (lower row) 12,000 years of model simulation. Scores are obtained as a product of normalized root mean square deviations from present-day ice thickness and ice speed, deviations in grounded and floating areas and grounding line positions, in line with the approaches presented in (Pollard et al., 2016; Albrecht et al., 2020). A focus is laid on the Amundsen Sea, Filchner-Ronne and Ross ice shelves by testing for those regions in particular. The individual scores are normalized to their median value with smaller scores indicating better fit with observations. The ensemble was done for PICO's heat exchange coefficient (left panels), PICO's overturning coefficient (middle panels) and the minimum till friction angle of the parameterized basal till properties (right panels). After 5,000 years, the best 5 simulations were continued and re-scored after 12,000 years to select the best ensemble member, shown in blue here with the state after the historic simulation shown in light blue.

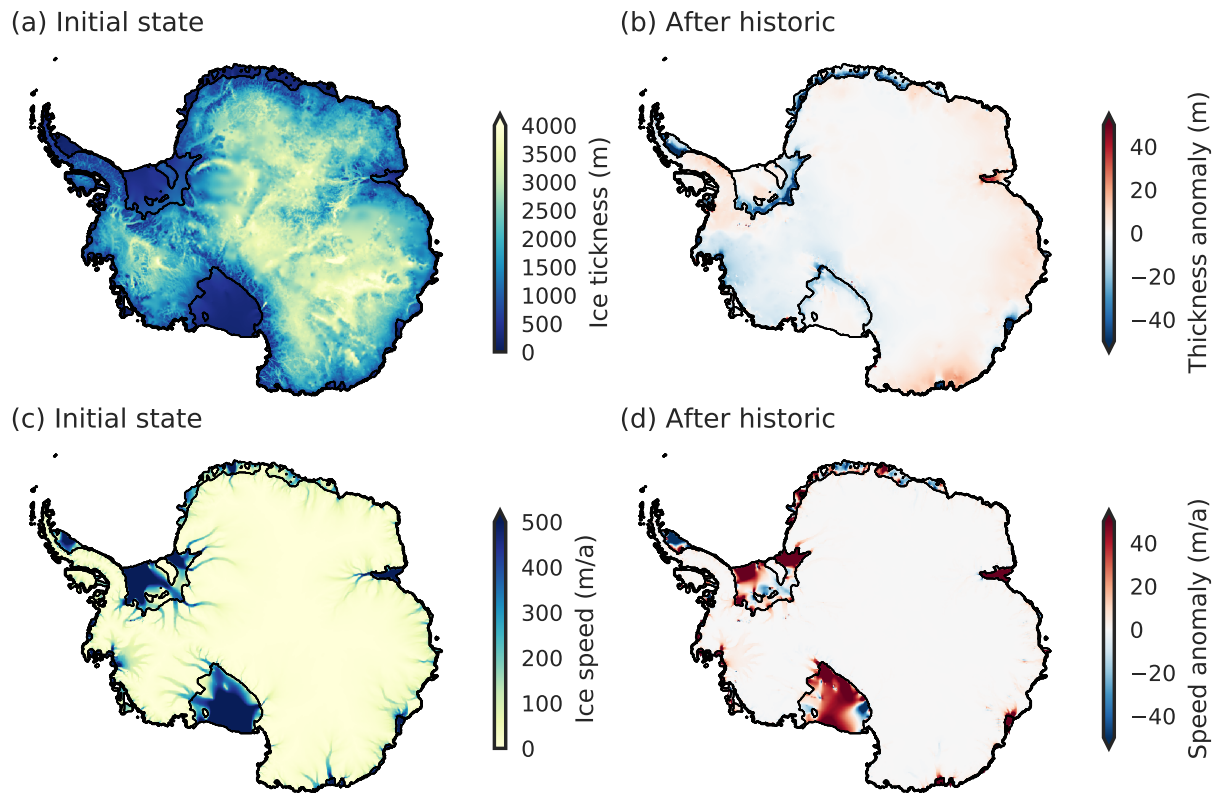


Figure S.2. ~~Modelled~~-~~Modeled~~ ice thickness as in (a) present-day pseudo-equilibrium configuration, and (b) changes after the historic run. Simulated ice speed in (c) pseudo-equilibrium and (d) changes after the historic run. Black contours indicate the initial (a,c) and final (b,d) grounding line location.

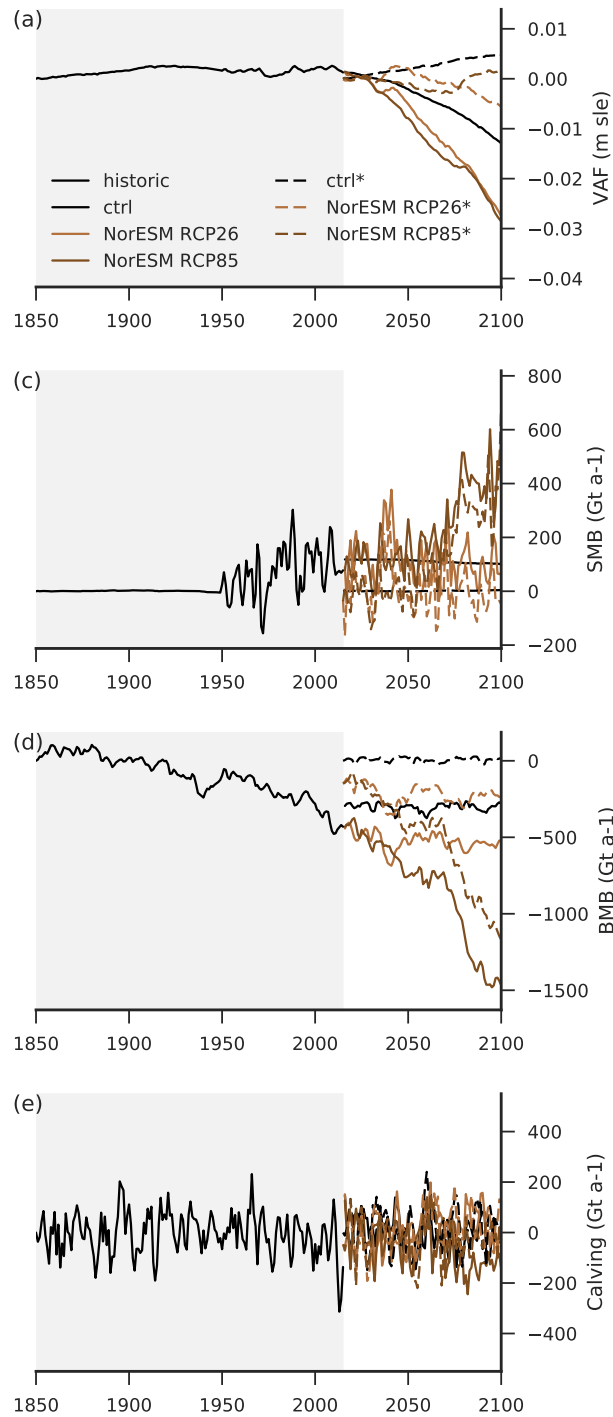


Figure S.3. ISMIP6 experiments with (solid lines) and without (dashed lines) historic initialisation. Shown is the evolution of the (a) volume above flotation, (b) surface mass balance, (c) basal mass balance and (d) calving flux at the ice front relative to the starting condition. Experiments are forced with changes in ocean temperature and salinity and surface mass balance and temperatures from the ISMIP6 protocol experiments no. 1 and 3.

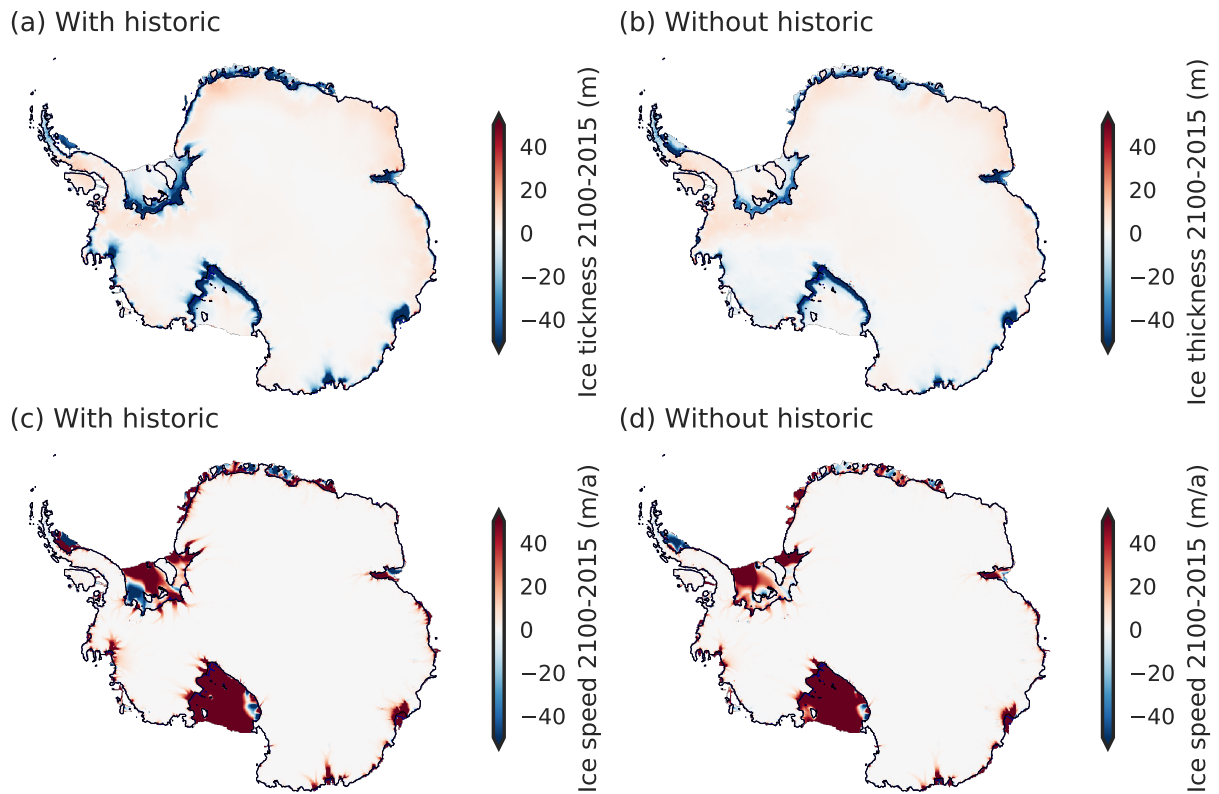


Figure S.4. Changes in ice thickness (a) with and (b) without the historic run between 2100 and 2015. The corresponding changes in ice speed (c) with and (d) without the historic run for experiment no. 1 from ISMIP6 (NorESM1-M, RCP8.5).

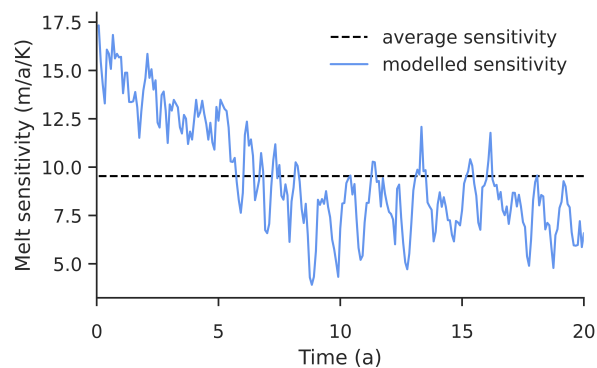


Figure S.5. [Sensitivity of sub-shelf melt rates of Thwaites glacier in the coupled simulation from Seroussi et al. \(2017\).](#) The sensitivity is estimated from the shelf-wide average melt rate in two coupled simulations that differ by initial and boundary ocean temperatures of 0.5°C . The sensitivity might be biased by differently evolving ice-shelf cavities over time.

Table S.1. List of all experiments, with INIT being based on the historic simulation starting from INIT*.

<u>MIP</u>	<u>INIT</u>	<u>INIT*</u>
		<u>historic ctrl</u>
		<u>historic</u>
<u>all</u>	<u>ctrl</u>	<u>ctrl*</u>
<u>initMIP</u>	<u>asmb</u>	<u>asmb*</u>
<u>initMIP</u>	<u>abmb</u>	<u>abmb*</u>
<u>ISMIP6</u>	<u>NorESM RCP85</u>	<u>NorESM RCP85*</u>
<u>ISMIP6</u>	<u>MIROC RCP85</u>	<u>MIROC RCP85*</u>
<u>ISMIP6</u>	<u>NorESM RCP26</u>	<u>NorESM RCP26*</u>
<u>ISMIP6</u>	<u>CCSM4 RCP85</u>	<u>CCSM4 RCP85*</u>
<u>LARMIP-2</u>	<u>AP 4m a⁻¹</u>	<u>AP 4m a⁻¹</u>
<u>LARMIP-2</u>	<u>EAIS 4m a⁻¹</u>	<u>EAIS 4m a⁻¹</u>
<u>LARMIP-2</u>	<u>RS 4m a⁻¹</u>	<u>RS 4m a⁻¹</u>
<u>LARMIP-2</u>	<u>AS 4m a⁻¹</u>	<u>AS 4m a⁻¹</u>
<u>LARMIP-2</u>	<u>WS 4m a⁻¹</u>	<u>WS 4m a⁻¹</u>
<u>LARMIP-2</u>	<u>AP 8m a⁻¹</u>	<u>AP 8m a⁻¹</u>
<u>LARMIP-2</u>	<u>EAIS 8m a⁻¹</u>	<u>EAIS 8m a⁻¹</u>
<u>LARMIP-2</u>	<u>RS 8m a⁻¹</u>	<u>RS 8m a⁻¹</u>
<u>LARMIP-2</u>	<u>AS 8m a⁻¹</u>	<u>AS 8m a⁻¹</u>
<u>LARMIP-2</u>	<u>WS 8m a⁻¹</u>	<u>WS 8m a⁻¹</u>
<u>LARMIP-2</u>	<u>AP 16m a⁻¹</u>	<u>AP 16m a⁻¹</u>
<u>LARMIP-2</u>	<u>EAIS 16m a⁻¹</u>	<u>EAIS 16m a⁻¹</u>
<u>LARMIP-2</u>	<u>RS 16m a⁻¹</u>	<u>RS 16m a⁻¹</u>
<u>LARMIP-2</u>	<u>AS 16m a⁻¹</u>	<u>AS 16m a⁻¹</u>
<u>LARMIP-2</u>	<u>WS 16m a⁻¹</u>	<u>WS 16m a⁻¹</u>

AP = Antarctic Peninsula, EAIS = East Antarctica, RS = Ross Sea, AS = Amundsen Sea, WS = Weddell Sea as specified in (Levermann et al., 2020).

Table S.2. Comparison of the PISM-PIK LARMIP-2 contribution and the PISM-PIK ISMIP6 contributions.

	<u>ISMIP6</u>	<u>LARMIP-2</u>
<u>horizontal resolution</u>	<u>8</u>	<u>4</u>
<u>vertical resolution</u>	<u>13-100m</u>	<u>7-48m</u>
<u>initialisation</u>	<u>steady-state, historic</u>	<u>600a constant climate</u>
<u>sub-grid friction at the GL</u>	<u>yes</u>	<u>yes</u>
<u>sub-grid melt at the GL</u>	<u>yes</u>	<u>no</u>
<u>basal melt rates</u>	<u>PICO</u>	<u>PICO</u>
<u>atmosphere</u>	<u>RACMOv2.3</u>	<u>RACMOv2.3</u>
<u>ocean</u>	<u>WOA18+SCH14</u>	<u>SCH14</u>
<u>Amundsen temperature</u>	<u>-1.25</u>	<u>-0.37</u>
<u>till friction angle</u>	<u>parameterized (ensemble)</u>	<u>optimized</u>
<u>eigencalving</u>	<u>$K = 1 \times 10^{16}$ms</u>	<u>$K = 1 \times 10^{17}$ms</u>
<u>thickness calving</u>	<u>threshold < 50m</u>	<u>threshold < 200m</u>
<u>prescribed maximum extent</u>	<u>Bedmap2</u>	<u>none</u>
<u>sliding law</u>	<u>pseudo-plastic exponent $q = 0.75$</u>	<u>plastic ($q = 0$)</u>

References: RACMOv2.3 (Van Wessem et al., 2018), WOA18 (Locarnini et al., 2018), SCH14 (Schmidtke et al., 2014).

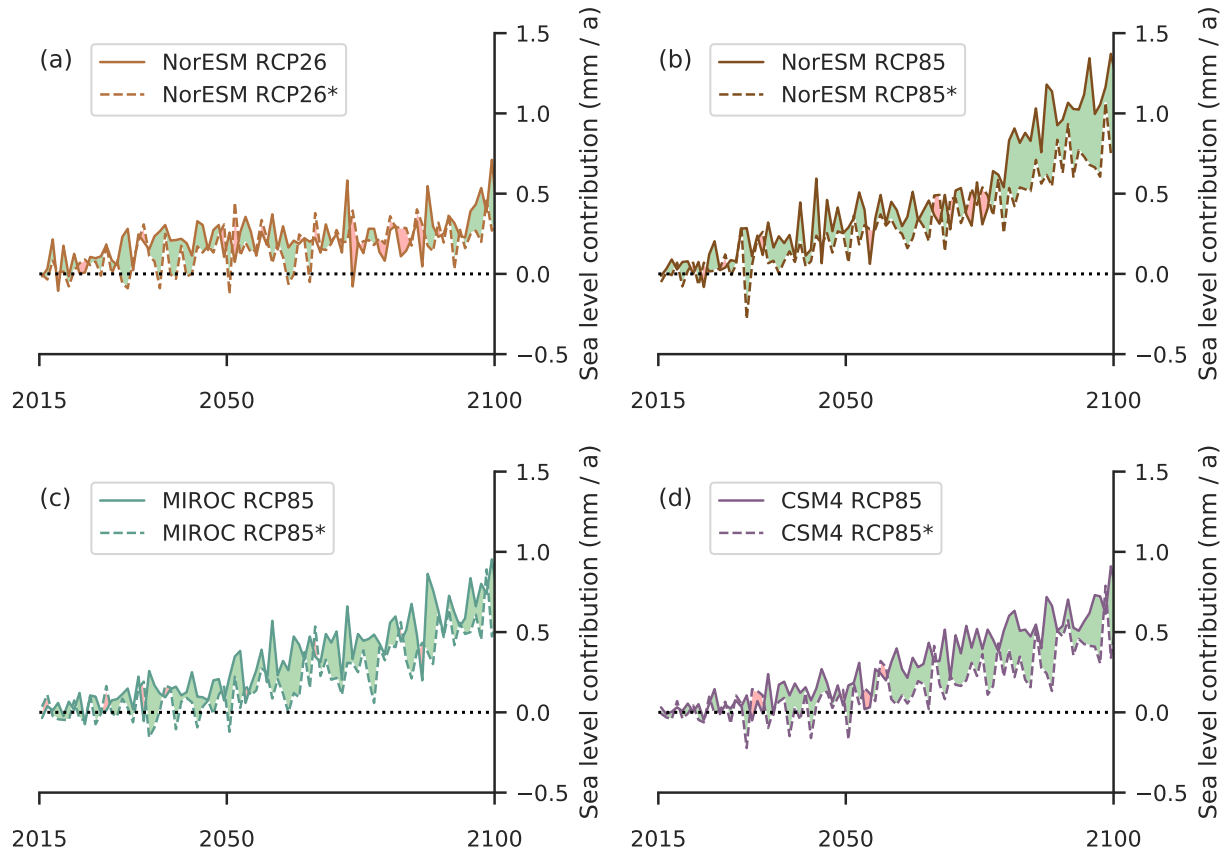


Figure S.6. Rate of sea-level rise between 2015 and 2100. We compare rates of sea-level rise for simulations driven by GCM ocean forcing with the corresponding model specified in the legend. Time periods when sea-level rates are larger in the simulations based on the historic simulation are indicated in green and periods when the simulations starting from the pseudo-steady state induce stronger sea-level rise are indicated in red.